Interfaces and fluctuations in confined polymeric liquid mixtures: from immiscible to near critical systems

2007 J. Phys.: Condens. Matter 19 073102

(http://iopscience.iop.org/0953-8984/19/7/073102)

INSTITUTE OF PHYSICS PUBLISHING JOURNAL OF PHYSICS: CONDENSED MATTER

J. Phys.: Condens. Matter **19** (2007) 073102 (34pp) doi:10.1088/0953-8984/19/7/073102

TOPICAL REVIEW

Interfaces and fluctuations in confined polymeric liquid mixtures: from immiscible to near critical systems

Michele Sferrazza[1,3] **and Clara Carelli**[2]

[1] Département de Physique, Université Libre de Bruxelles, Boulevard du Triomphe CP223, 1050 Bruxelles, Belgium
[2] Ecole Supérieure de Physique et Chimie Industrielles (ESPCI), Paris, France

E-mail: msferraz@ulb.ac.be

Received 23 November 2006, in final form 10 December 2006
Published 23 January 2007
Online at stacks.iop.org/JPhysCM/19/073102

Abstract

In this paper the structure of the interface between polymer films is discussed to elucidate fluctuations and confinement effects in fluid polymer mixtures. The neutron reflectivity technique has been employed to investigate the dependence of the structure of the interface on the degree of immiscibility of the polymers over a wide range, as criticality is approached, and to characterize it in terms of intrinsic width, as calculated by mean field theories, and capillary fluctuations. For more immiscible systems, as the degree of incompatibility between the polymers is decreased, the width of the interface increases slowly, and it is independent of the molecular weight of the polymers. Closer to the critical point the dependence on the degree of miscibility becomes stronger and the way in which the interfacial width diverges, as criticality is approached, is related to both chain length and Flory–Huggins interaction parameter (χ). The results have been compared to the predictions of mean field theories. Self-consistent field numerical calculations, with the additional contribution due to capillary waves, provide a good description of the width of the interface between two polymer bulk phases, in particular at higher and intermediate degrees of immiscibility—the product of the Flory–Huggins interaction parameter χ and the number N of monomers of the chain, χN. For more miscible systems a crossover is observed to a region where the square gradient theory in the weak segregation limit better approximates the experimental results.

Moreover, the mechanisms by which confinement affects the interface have been investigated. To understand the relative importance of the long ranged van der Waals forces and short ranged 'truncation forces' in modifying thermally excited fluctuations at the polymer/polymer interface, the thickness dependence of the interfacial width has been studied for different degrees of miscibility, approaching criticality. The results show a gradual transition from a region where long ranged dispersion forces are dominant in influencing the capillary

[3] Author to whom any correspondence should be addressed.

wave spectrum, for higher degrees of immiscibility, to a region where short ranged forces—connected to the presence of the walls—become more important and the dependence of the interfacial width on film thickness is stronger. The thickness dependence of the interfacial width was also studied for systems with different molecular weights in different conditions of miscibility, to investigate the effects of a confined geometry on polymers with different chain lengths as criticality is approached.

(Some figures in this article are in colour only in the electronic version)

Contents

1. Introduction

The problem of the structure of the interface between two coexisting fluid phases has a long history, dating back to van der Waals [1], but there has been a recent burgeoning of theoretical work in this area, particularly in relation to the effects of confinement and reduced dimensionality on fluid phase behaviour. Phenomena related to wetting and capillary condensation, for example, have fundamental interest in the area of phase transitions in situations of reduced dimensionality, with strong analogies to magnetic transitions in thin films. This issue touches on many technologically important problems, for example the behaviour of fluid mixtures in porous media, and the formation of self-stratified industrial coatings. The experimental effort has been a lot smaller than the theoretical one, largely because the study of the structure of interfaces between two coexisting fluids and the control of the strength of surface fields in confining geometries present difficult experimental problems. However, one subset of fluid mixtures has proved very fruitful for experiments—coexisting polymeric liquids, where the technique of neutron reflectivity has proved invaluable for probing the structure of interfaces with sub-nanometre resolution [2].

The problem of the structure of the interface between two immiscible polymers, both in bulk and in thin films, is, of course, of considerable technological relevance in its own right; this interface controls the level of adhesion in multicomponent blends and thus their bulk mechanical properties. The level of adhesion between a thin polymer layer and a polymer substrate is important in coating technology, while in new polymer semiconducting devices for optoelectronics applications interfaces between different polymers control device performance. A number of recent studies on polymer thin films have identified novel phenomena or effects that in principle have a more general applicability to other types of fluid mixtures. Examples include the discovery of surface directed spinodal decomposition [3], studies of the kinetics of growth of wetting layers [4], and the study of finite size effects on interfacial width in thin films, which has helped to understand the contribution made by capillary wave fluctuations in broadening the intrinsic interfacial width between immiscible polymers [5].

In addition to the specific technological interest of polymer thin films there are compelling reasons to consider them among the most ideal and convenient exemplars for general fundamental studies of phase behaviour in confined films [6]. These advantages include their relatively long natural length scales, set by the radius of gyration of the chain. These make experiments more convenient and simplify theoretical interpretation; the clear separation of length scales between the molecular and the atomic makes continuum theories particularly powerful. Polymers are characterized by slow timescales, and in many cases it is easy and convenient to quench samples into a glassy state; together, these factors allow one to probe the dynamics of the approach to equilibrium and permit the study of metastable states. Polymers have an extra control parameter compared to small molecule liquids—the degree of polymerization. This is of fundamental importance, as it determines the relative importance of concentration fluctuations. For high molecular weight polymers mean field theory works well, while bulk fluctuation effects become more important at lower degrees of polymerization. In some cases—isotopic blends—there is a very well defined interaction between the components, arising from pure dispersion forces and strict structural symmetry between components. Finally, polymers have a number of practical advantages—spin coating allows one reproducibly to prepare highly uniform, smooth films with thicknesses down to a few nanometres, while well known film handling techniques allow one to prepare non-equilibrium starting structures such as bilayers with interfaces sharp at the sub-nanometre level. Polymers are also very well suited, because of the possibility of deuterium labelling, to the use of specular and off-specular neutron reflectivity, which are the ideal techniques to study interfaces in polymer thin films and to characterize in plane structures [7]. This powerful tool can also be backed up by laboratory based techniques such as atomic force microscopy, and x-ray reflectivity.

In order to realize the full advantages of polymer systems as model systems for studying fluid interfaces and critical phenomena in confined geometries, it is necessary to be able to use ideal model systems. Advances in control of microstructure during anionic polymerization combined with a recent comprehensive body of work on the bulk thermodynamics of polyolefin mixtures [8] allowed us to study confined thin polymer films with a unique class of polymers, well defined systems, whose interaction parameters can be tuned at will. This gives us an unparalleled degree of control over the polymers' miscibility in our experiments. Although this class of materials is important due to their attractiveness from the physicist's point of view of being able to control the interactions between the components, they also have considerable technological relevance. New advances in metallocene catalysis have led to the bulk commercial availability of a wide variety of polyolefins of controlled chain architecture, and hydrogenated polybutadienes turn out to be very good models for some of these important new materials [9].

The aim of this paper is to present our understanding of the structure of thin films of mixtures of very well controlled polymers, characterizing the nature of the interface between the coexisting phases, using neutron reflectivity. The issues include the following.

(1) How does the width of the interface depend on the distance away from the critical point?
The interface between two immiscible polymers is not atomically sharp but is characterized by a well defined width, determined by a balance of chain entropy and energetic interaction between the polymer chains. For systems with a high degree of immiscibility (the product of the degree of polymerization and the interaction parameter) the interfacial region is narrow, while closer to the critical point the interface becomes indefinitely wide. For strongly immiscible systems the self-consistent field (SCF) theory, in the limit of strong segregation, could be used to predict analytically the interfacial width. As the degree of incompatibility is decreased the SCF theory becomes inaccurate and square gradient theories could be used to determine the interfacial structure (the weak segregation limit), but the way the two approaches cross over is not well characterized.
Criticality can be achieved at low molecular weight with larger segment–segment interaction parameter or at high molecular weight with a smaller segment–segment interaction parameter. At high molecular weights mean field theories could be used to describe the thermodynamics of the interface: the divergence of the interfacial width approaching criticality will be characterized in this case by mean field exponents. In more strongly interacting systems, whose critical point occurs for lower degrees of polymerization, we should cross over to non-classical exponents and the mean field approach should be reconsidered.
The existing data are limited to demonstrating the divergence near the critical point qualitatively [10]. Quantitative tests of the character of the divergence, and on the crossover from weak to strong segregation limits, are presented.

(2) How is the nature of the interface modified by interfacial fluctuations, and how is this modified by confinement effects in thin films?
It is now clear that the equilibrium interface width in polymer systems is substantially broader than the mean field prediction, and that the origin of this broadening is thermally excited capillary waves. It is also clear that in confined systems the spectrum of capillary waves is modified, and that this has a substantial effect on their contribution to interfacial width in thin films. However, there is controversy in the literature about the relative importance of long range van der Waals forces [5] and short range 'truncation forces' [11] in influencing the capillary wave spectrum. Recent simulations make it clear that in principle both should be taken into account [12]; in order to untangle this issue systematic experiments are presented to investigate the confinement effect on interfacial width on a series of samples in which the degree of incompatibility is kept constant while the degree of polymerization is changed; it is the latter parameter which determines how strong the short range interaction is.

2. Interface width in immiscible and quasi-miscible polymers

In the last years there has been a large burgeoning of theoretical studies in the area of polymer/polymer interfaces [2, 6, 13–21], due to the critical role that the properties of these interfaces play in technology. Two different theoretical approaches have been developed to describe the structure of the interface between two incompatible polymers. The self-consistent field method provides analytical expressions for the width of the interface and the interfacial tension for strongly immiscible polymers, in the limit of chains with infinite lengths (strong

segregation limit) [2, 14, 18]. On the other hand, in the vicinity of the critical point, where the volume fraction of the polymers at the interface varies slowly, the square gradient theory can be used to predict analytically the interfacial profile (weak segregation limit) [13, 15]. However the way these two approaches cross over, as criticality is approached, is not known. Recently computer simulations have also become a major tool to study polymer/polymer interfaces, complementing analytical theories [19]. Numerical methods and Monte Carlo simulations have been developed to solve exactly systems of SCF differential equations [6, 13, 22–25], and to calculate a composition profile across the interface. However, due to the limited power of workstations, computer simulations restrict their attention to polymers with very short chains, thus questions regarding the effect of parameters such as the degree of polymerization cannot be directly addressed [19].

To compare theory and simulations with experimental results on polymer interfaces, the contribution of capillary waves needs to be considered [1, 26]. These fluctuations of the local position of the interface broaden the apparent interfacial width. The measured interface will then depend on the lateral resolution, and can be modified by external forces that affect the capillary waves, such as gravity or van der Waals interactions [1].

Interfaces between different polymer systems have been investigated experimentally, including amorphous homopolymers [27, 28, 5, 29], copolymers [10, 11, 30], crystalline and semi-crystalline polymers [31, 32]. The experimental results have been reviewed by Stamm and Schubert [33] and by Jones [34]. One of the most extensively studied blends is the strongly immiscible polymer pair deuterated-polystyrene/poly(methyl-methacrylate) (dPS/PMMA). Neutron reflectivity experiments by different groups have found that the width of the interface between the two bulk phases is 50 Å [5, 27, 28]. This result was independent of the molecular weight of the polymers and of the temperature at which the samples were annealed to allow the interface to reach equilibrium. More recent experiments on the same system enabled the understanding of the substantial effect of capillary waves in determining the overall structure of an interface [5].

More miscible systems have been investigated with nuclear reaction analysis (NRA). Experiments on the pair polystyrene/deuterated-polystyrene (hPS/dPS), for example, have shown that the width of the interface, at temperatures below the critical temperature for phase separation, grows with time up to a limiting value [10]. The measured interfacial width is in qualitative agreement with the prediction of the square gradient theory for quasi-miscible systems.

Despite the number of experiments on polymer/polymer interfaces, a complete study of the dependence of the interfacial profile on the entire range of conditions of miscibility is missing. One of the questions still open in this field concerns the relative importance of intrinsic interfacial width, as calculated by mean field theories, and capillary waves, in determining the overall structure of an interface as criticality is approached. The aim of the experimental work described in section 10 was to address this issue, performing a systematic study of the interface between polymer phases as a function of the degree of immiscibility χN. Quantitative tests of the theory will be reported, to determine the accuracy of the self-consistent field theory and to characterize the crossover from the strong to the weak segregation limit, where the square gradient theory is valid.

3. The self-consistent field theory

The problem of the conformation of a polymer chain that is interacting with many other chains presents a remarkable analogy with the classical problem of the electronic structure of atoms with many electrons, which can be solved by using the Hartree method. This idea, originally

pointed out by Edwards, is at the base of the self-consistent field (SCF) theory proposed in 1971 by Helfand and Tagami, in order to determine the width of the interface and the interfacial tension between two immiscible polymer phases [14]. This approach considers a polymer chain at the interface as a random walk in a chemically inhomogeneous environment. The walk is affected by a mean field potential, resulting from the interaction with all the other polymer chains. The first step in the SCF method is the definition of a distribution function $q(r, r', t)$, that represents the probability that a chain with t segments starts at a position r and finishes at r'. Each polymer chain can then be described by the following equation [2]:

$$\frac{\partial q(r, r', t)}{\partial t} = \frac{a^2}{6}\nabla^2 q(r, r', t) - \frac{U(r)}{kT}q(r, r', t) \tag{1}$$

where a is the characteristic segment length of the polymer, k the Boltzmann constant and T the temperature. $U(r)$ is a spatially varying potential defined as [2]

$$U(r) = \chi(1 - \varphi(r)) + w(r). \tag{2}$$

In equation (2) the first term describes the energetic interaction between different monomers, while the second part, expressed as the function $w(r)$, arises from the assumption of incompressibility of the system. In the case of a planar interface, where only the z component is important, the equations for the distribution functions in the case of two immiscible polymers, A and B, are given by

$$\frac{\partial q_{\mathrm{A}}(z, t)}{\partial t} = \frac{a^2}{6}\nabla^2 q_{\mathrm{A}}(z, t) - \frac{U_{\mathrm{A}}(z)}{kT}q_{\mathrm{A}}(z, t) \tag{3}$$

and

$$\frac{\partial q_{\mathrm{B}}(z, t)}{\partial t} = \frac{a^2}{6}\nabla^2 q_{\mathrm{B}}(z, t) - \frac{U_{\mathrm{B}}(z)}{kT}q_{\mathrm{B}}(z, t). \tag{4}$$

The volume fractions $\varphi_{\mathrm{A}}(z)$ and $\varphi_{\mathrm{B}}(z)$ are then related to the distribution functions by the following equations:

$$\varphi_{\mathrm{A}}(z) = \frac{1}{N}\int_0^N \mathrm{d}t\, q_{\mathrm{A}}(z, N - t)q_{\mathrm{A}}(z, t) \tag{5}$$

and

$$\varphi_{\mathrm{B}}(z) = \frac{1}{N}\int_0^N \mathrm{d}t\, q_{\mathrm{B}}(z, N - t)q_{\mathrm{B}}(z, t) \tag{6}$$

where N represents the total number of segments in the polymer chain.

Since each polymer molecule at the interface obeys equations (3) and (4), the result is a system of coupled differential equations, the solution of which requires the use of numerical methods [25]. However, for two strongly immiscible polymers, in the limit of infinite molecular mass ($N \to \infty$) (strong segregation limit), there is an analytical solution. In this case all the segments along the polymer chain are equivalent and equations (5) and (6) can be replaced by the simple expressions

$$\varphi_{\mathrm{A}}(z) = q_{\mathrm{A}}^2(z) \tag{7}$$

and

$$\varphi_{\mathrm{B}}(z) = q_{\mathrm{B}}^2(z). \tag{8}$$

For the specific boundary conditions $\varphi_{\mathrm{A}}(z \to -\infty) = 0$ and $\varphi_{\mathrm{A}}(z \to \infty) = 1$, the volume fraction of the polymer A across the interface, $\varphi_{\mathrm{A}}(z)$, is then given by the

following function (more precise details on the derivation of equation (9) can be found in the literature) [2, 6, 13, 21]:

$$\varphi_{\mathrm{A}}(z) = \frac{1}{2}\left[1 + \tanh\left(\frac{z}{w_{\mathrm{I}}}\right)\right] \tag{9}$$

where z represents the distance from the mean point of the interface, and w_{I}, known as the intrinsic interfacial width, is defined as

$$w_{\mathrm{I}} = \frac{a}{\sqrt{6\chi}}. \tag{10}$$

In equation (10), a is the characteristic segment length of the polymers.

The interfacial tension γ between the two phases is given by the expression

$$\gamma = k_{\mathrm{B}} T \rho a \sqrt{\frac{\chi}{6}} \tag{11}$$

where ρ is the density of the polymers, a is the characteristic segment length, k_{B} is the Boltzmann constant and T is the temperature.

Measured values of the polymer–polymer interfacial width, obtained with the neutron reflection technique for various types of polymer interfaces, ranging from block copolymers to polymer brushes in polymer matrices, are typically higher than the values extracted from the self-consistent field theory [33, 34]. A possible explanation for this discrepancy has been suggested: the experimental result agrees with the theoretical prediction if a correction to the interfacial width due to capillary wave fluctuations is considered [5].

3.1. Effects of chain length

In equation (10), w_{I} represents the intrinsic interfacial width in the strong segregation limit for the approximation of infinite chain lengths.

In general, to consider finite molecular mass, Tang and Freed suggested the following formulae for w_{I} and the interfacial tension, γ, that have been shown to be in good agreement with the numerical calculations of the SCF theory [18]:

$$w_{\mathrm{I}} = \frac{a}{\sqrt{6\chi}}\left[\frac{3}{4}\left(1 - \frac{2}{\chi N}\right) + \frac{1}{4}\left(1 - \frac{2}{\chi N}\right)^2\right]^{-1/2} \tag{12}$$

$$\gamma = k_{\mathrm{B}} T \rho a \sqrt{\frac{\chi}{6}}\left(1 - \frac{1.8}{\chi N} - \frac{0.4}{(\chi N)^2}\right)^{3/2} \tag{13}$$

where ρ is the density of the polymer, k_{B} the Boltzmann constant and T the temperature.

As can be observed in equations (12) and (13), the corrections to the values obtained in the strong segregation limit depend only on the inverse degree of immiscibility, $(\chi N)^{-1}$, and become important only for polymer pairs close to criticality. Thus the interfacial width varies mainly with $\chi^{-1/2}$ while the interfacial tension γ depends on the square root of the interaction parameter.

It should be pointed out that these results are obtained under the assumption that the density and the statistical segment lengths of the two polymers are identical. If this approximation is removed, more complicated expression can be derived for w_I and γ [35].

4. The weak segregation limit

The SCF theory provides analytical expressions for the width of the interface and the interfacial tension between strongly immiscible polymer pairs. However, for more miscible systems the

approximation of strong segregation of the two polymer phases is not valid anymore. In this case, the theory proposed by Cahn and Hilliard can be used to predict the interfacial width [15]. This approach is based on the assumption that the number of configurations available for a polymer chain at the interface is reduced by the presence of a gradient in the composition. The free energy is then given by the sum of two terms [13]: the Flory–Huggins free energy $F_{\mathrm{FH}}(\varphi)$ for a homogeneous mixture of the two polymers and a second term proportional to the square of the composition gradient $(\nabla\varphi)^2$. The final form for the free energy per segment for an inhomogeneous system, known as the square gradient expression, is

$$F_{\mathrm{SQ}} = k_{\mathrm{B}}T \int [F_{\mathrm{FH}}(\varphi) + \kappa(\varphi)(\nabla\varphi)^2]\,\mathrm{d}r. \tag{14}$$

The gradient coefficient $\kappa(\phi)$ is given by

$$\kappa(\varphi) = \frac{\chi r_0^2}{6} + \frac{a^2}{36\varphi(1-\varphi)} \tag{15}$$

where the first term represents the intermolecular interactions in a range defined by the distance r_0 of the order of a few nanometres [16], while the second term describes the entropic effects due to the restriction of possible configurations for the chain (a is the statistical segment length and $\varphi_{\mathrm{A,B}}$ are the volume fractions of polymer A and B respectively). This phenomenological approach is valid in the limit of relatively small concentration gradients, a condition verified only for weakly immiscible polymer pairs. Numerical methods can be used in order to find a concentration profile that minimizes the free energy. However, close to the critical point, where the concentration varies slowly on the scale of the radius of gyration (weak segregation limit) [2], there is an analytical solution given by

$$\varphi(z) = \frac{1}{2}\left[\varphi_1 + \varphi_2 + (\varphi_2 - \varphi_1)\tanh\left(\frac{z}{w_{\mathrm{crit}}}\right)\right] \tag{16}$$

where φ_1 and φ_2 are two coexisting compositions that define the boundary conditions in the system, and z represents the spatial dimension perpendicular to the interface. The critical interfacial width, w_{crit}, and the interface tension, γ_{crit}, are given in this case by

$$w_{\mathrm{crit}} = \frac{a\sqrt{N}}{3}\left(\frac{\chi}{\chi_{\mathrm{crit}}} - 1\right)^{-1/2} \tag{17}$$

and

$$\gamma_{\mathrm{crit}} = \frac{9k_{\mathrm{B}}T}{a^2\sqrt{N}}\left(1 - \frac{\chi_{\mathrm{crit}}}{\chi}\right)^{3/2} \tag{18}$$

where χ_{crit} represents the value of F–H interaction parameter at the critical point. Equations (17) and (18) show that at the critical point the width of the interface diverges while the interfacial tension goes to zero. Although this theory gives an estimation of w and γ for weakly immiscible polymers, it is not particularly accurate very close to the critical point, where fluctuations in the composition become more important and the mean field approach should be reconsidered [1]. As observed by De Gennes, polymer blends can exhibit Ising-like critical properties. However the long ranged nature of polymer–polymer interactions reduces the Ising regime to a very narrow range [36–38]. According to the Ginzburg criterion the limit of the mean field approximation [2], or in other words how close to the critical point one needs to be for these fluctuations to become relevant, is defined by the condition

$$\left|\frac{\chi}{\chi_{\mathrm{crit}}} - 1\right| \leqslant \frac{1}{N}. \tag{19}$$

From equation (19) it follows that in the case of high molecular weight polystyrene and deuterated polystyrene, for example, concentration fluctuations must be taken into account only when the distance from the critical point is lower than 0.05 °C.

5. Interfacial fluctuations

Mean field theories should describe well the interfacial width between immiscible polymer blends. However, different experiments on immiscible polymer pairs have found discrepancies between the experimental results and the theoretical predictions of the SCF theory: the measured interfacial width was broader than the one estimated theoretically [27–29]. This difference has been attributed to the presence of capillary waves at the interface [26, 39]. These are thermally excited fluctuations of the local position of the interface, present at all fluid interfaces [40, 41]. The interface between two immiscible polymers can then be imagined as a bare interface with width $2w_{\mathrm{I}}$, roughened by the presence of capillary waves.

In general, the dividing surface between the two fluid phases, $\varsigma(x, y)$, can be represented as the sum of surface waves [1]:

$$\varsigma(x, y) = \sum_k A(q) \mathrm{e}^{\mathrm{i}\vec{q}\cdot\vec{s}} \tag{20}$$

where $\vec{s}$ represents a vector in the (x, y) plane, while $\vec{q}$ and $A(q)$ are, respectively, the wavevector and the amplitude of each capillary wave. Each wave creates a surface area with free energy $\frac{1}{4}A(q)^2q^2S\gamma$, S being the total area of the flat interface and γ the interfacial tension. Making use of the theorem of equipartition of the energy, at equilibrium the average value of the energy associated with the additional surface is $\frac{1}{2}k_{\mathrm{B}}T$. The mean square value of the amplitude of capillary waves is then given by [2]

$$\langle A(q)^2\rangle = \frac{8k_{\mathrm{B}}T}{Sq^2\gamma}. \tag{21}$$

The contribution of capillary waves to the interface can be calculated by integrating the mean square capillary wave dispersion σ_ς^2 due to all the possible waves:

$$\sigma_\varsigma^2 = \langle \varsigma^2 - \langle\varsigma\rangle^2\rangle = \int \frac{k_{\mathrm{B}}T}{2\pi\gamma}\frac{\mathrm{d}q}{q}. \tag{22}$$

In principle all the values are possible for the wavevector q, thus the integral of equation (22) diverges and the position of the interface is not defined thermodynamically. There must therefore be physical limits to the wavelengths, and the mean squared dispersion of capillary waves obtained by integrating equation (22) can be written as

$$\sigma_\varsigma^2 = \frac{k_{\mathrm{B}}T}{2\gamma\pi}\ln\frac{q_{\max}}{q_{\min}} \tag{23}$$

where $q_{\min}$ and $q_{\max}$ represent the lower and upper cut-off for capillary wavevectors. The maximum value of q is related to a minimum length defined for the system, such as the intrinsic width w_{I} of the interface. A detailed analysis by Semenov shows that the effective $q_{\max}$ is indeed given by $1/(\pi w_{\mathrm{I}})$ [39].

The definition of $q_{\min}$ is instead more complex. The lowest possible wavevector can be related for example to the lateral size of the system: the wavelengths cannot in fact exceed the size of the sample. However, other factors may determine a different cut-off, for example the lateral resolution of the technique used to measure the interface or an external force.

In general an external potential $v(z)$ will introduce a cut-off q_{ext} given by

$$q_{\mathrm{ext}} = \left(\frac{1}{\gamma}\left(\frac{\partial v(z)}{\partial z}\right)\right)^{1/2}. \tag{24}$$

For instance, gravity introduces a lower cut-off on the spectrum characterized by a gravitational capillary length a_{grav} given by [1]:

$$a_{\mathrm{grav}} = \sqrt{\frac{2\gamma}{g\Delta\rho}} \tag{25}$$

where $\Delta\rho$ is the difference in the mass density between the two phases. For polymer/polymer interfaces this length is of the order of millimetres [5], thus in these systems wavelengths longer than a few millimetres will not be considered.

Hence the total interfacial width measured experimentally, $2w$, can be considered as composed by two terms related to the intrinsic width w_{I} and to the capillary wave component σ_ς, added in quadrature:

$$2w = (4w_{\mathrm{I}}^2 + 2\pi\sigma_\varsigma^2)^{1/2}. \tag{26}$$

It should be pointed out that the experimental width not only depends on the conditions of miscibility, but also on the dimension of the sample investigated, on the coherence length of the experimental technique and on external forces, that may modify the contribution of interfacial fluctuations to the interface.

6. Confinement effects on the interfacial fluctuations

As discussed in the previous section, the width of the interfaces between two polymer phases can be substantially influenced by potentials that affect the spectrum of capillary waves. For polymer thin films, two different behaviours have been observed experimentally that relate the size of the system to the interfacial width. Experiments on the strongly immiscible polymer pair polystyrene/poly(methyl-methacrylate) (PS/PMMA) showed that long ranged dispersion forces acting across a very thin film introduce a cut-off for small wavevectors, leading to a logarithmic dependence of the interfacial width on film thickness [5, 42, 43].

Instead, contrasting results were obtained from the investigation of a quasi-miscible polymer pair, close to the critical point: the lower cut-off for capillary wavevectors was determined in this case by the short ranged interactions between the polymer/polymer interface and the other film boundaries; the measured interfacial width was found to vary with the square root of the film thickness [11, 44].

Computer simulations of the thickness dependence of the interfacial profiles between two polymer phases confined between rigid walls suggest that both these forces in principle should be considered [23]; however, the mechanism by which the confined geometry affects the interfacial width is not fully understood. The effect of long and short ranged forces on the spectrum of capillary waves will be discussed in more detail in the next sections.

6.1. Long ranged dispersion forces

Van der Waals dispersion forces arise from the instantaneous dipole–dipole interaction between atoms or molecules [45]. These forces, characterized by being effective on long ranges, are always present, even between neutral systems, and play an important role in many physical phenomena, such as wetting, adhesion or absorption. In the case of an interface between two polymers, dispersion forces become important when one or both the phases are rather thin. When a thin layer is interposed between two semi-infinite media, for example a polymer substrate and another medium, there will be a van der Waals interaction between the two media across the film inversely proportional to the fourth power of the thickness of the layer d [5]:

$$F(d) \sim \frac{A}{d^4} \tag{27}$$

where A is the Hamaker constant. The dispersion force may lead to a cut-off for small wavevectors that suppresses capillary waves with wavelengths longer than a characteristic capillary length a_{dis}. As a result, the contribution of capillary waves to the interfacial width is reduced [5].

Making use of equation (24), the following expression can be derived for a dispersive length a_{dis} [5]:

$$a_{\mathrm{disp}} = \sqrt{\frac{4\pi\gamma d^4}{|A|}}. \tag{28}$$

As a result, for the interface between a polymer substrate and a thin film of thickness d, the value of $q_{\min}$ in equation (23) is equal to $2\pi/a_{\mathrm{disp}}$. The mean squared dispersion of capillary waves is then given by

$$\sigma_\zeta^2 = \frac{k_{\mathrm{B}}T}{2\gamma\pi}\ln\left(\frac{q_{\max}}{C_1}d^2\right) = \frac{k_{\mathrm{B}}T}{2\gamma\pi}\left(\ln\left(\frac{q_{\max}}{C_1}\right) + 2\ln d\right) \tag{29}$$

where the constant C_1 introduced is equal to $\left(\frac{\pi A}{\gamma}\right)^{1/2}$. Thus the measured interfacial width will vary logarithmically with the thickness of the film d, as observed in neutron reflectivity experiments by Sferrazza *et al* [5].

6.2. Short ranged 'truncation' forces

For quasi-miscible polymer pairs, and thus broader interfaces, another effect related to the finite size of the system needs to be taken into account. When the interfacial width is a considerable fraction of the thickness of the film, there will be short ranged interactions between the interface and the boundaries of the layer. A polymer molecule at the interface will be subject in this case to an effective potential that takes the form [46–48]

$$V(d) \propto \mathrm{e}^{-kd} \tag{30}$$

where d is the distance of the interface from the boundary surface. This surface field will have the effect of truncating the interfacial profile, by introducing a large correlation length ξ on interfacial fluctuations in the direction parallel to the plane of the interface, which increases exponentially with the thickness of the film d [49–51]:

$$\xi \approx \xi_{\mathrm{B}}\mathrm{e}^{kd/2}. \tag{31}$$

In equation (31), ξ_{B} represents the bulk correlation length [50] and k^{-1} is a transverse decay length. k is of the order of ξ_{B} for weakly immiscible polymer pairs, while it is better approximated by the interfacial width in the limit case of strongly segregated polymer mixtures [51]. ξ_{B} is defined by

$$\xi_{\mathrm{B}} = \frac{a}{6}\Big/\left(\frac{1-\phi}{2N_1} + \frac{\phi}{2N_2} - \chi\phi(1-\phi)\right)^{1/2} \tag{32}$$

where a is the statistical segment length, N_1 and N_2 are the degrees of polymerization of the two coexisting polymers, and ϕ is the coexistence composition [52].

The strong dependence of ξ on film thickness can be understood by considering that the 'truncation effect' is weak in thicker films, where the film boundaries are more distant from the mean position of the interface. For thinner films instead it becomes more important and the correlation length is smaller. As a result, the lower cut-off $q_{\min}$ is given by $2\pi/\xi$ and, neglecting long ranged forces, the capillary wave mean square dispersion σ_ζ^2 of equation (23) takes the form

$$\sigma_\zeta^2 = \frac{k_{\mathrm{B}}T}{2\gamma\pi}\ln\left(\frac{q_{\max}}{2\pi/\xi}\right) = \frac{k_{\mathrm{B}}T}{2\gamma\pi}\left(\ln\left(\frac{q_{\max}}{2\pi}\xi_{\mathrm{B}}\right) + \frac{kd}{2}\right). \tag{33}$$

It follows that, in the presence of short ranged forces, the contribution of capillary waves to the interfacial width σ_ζ^2 contains a term that is proportional to the film thickness d, as shown experimentally by Kerle *et al* [11].

In our work, by focusing on a system where we could change systematically the conditions of miscibility, and in consequence the width of the interface, we could fully investigate the effect of both long ranged dispersion forces, that lead to a logarithmic dependence of the interfacial width on the thickness, and short ranged interactions that involve a square-root dependence.

7. Neutron reflection

The interface between two immiscible polymers is typically smaller than 400/500 Å. The use of a technique to measure the interfacial width must therefore take into consideration this length scale. Moreover, a suitable contrast must be available between the two phases [53, 54].

Neutron reflectivity represents an ideal tool to probe polymer/polymer interfaces. This technique provides an excellent spatial resolution, down to 1 nm, thanks to the short wavelengths available for thermal neutrons. It also gives the possibility to investigate buried interfaces, due to the high penetrating power of neutrons, which enables an incident neutron beam to propagate in a solid medium before reaching an interface. This represents a great advantage for the study of, for example, solid–liquid interfaces [55]. In addition, the neutron beam produces less damage to a sample, allowing more successive measurements of the same sample.

The success of the application of neutron reflectometry to polymers arises from the fact that the scattering length density of materials can be altered by performing isotopic substitutions between hydrogen and deuterium. This allows one to generate a large contrast between polymer phases, and thus to be more sensitive to the interface.

Reflectivity experiments probe the mean change in the refractive index perpendicular to the interfaces. Thus, from the analysis of the specular neutron reflection on a thin film structure, we can obtain the one-dimensional scattering length density profile perpendicular to the surface, which can be directly related to the chemical profile.

The reflectivity is given by $R = |r|^2$, where r is the amplitude reflectance obtained by solving the one-dimensional Schrödinger equation in the direction perpendicular to the sample. If we have neutrons propagating from vacuum into a uniform material of scattering length density b/V, the perpendicular component of the wavevector within the material k_i is expressed by

$$k_i = \sqrt{k^2 - 4\pi \frac{b}{V}}. \tag{34}$$

In the case $4\pi b/V > k^2$, k is imaginary and then the neutrons propagate into the materials only as an evanescent wave, giving rise to total external reflection (reflectivity is unity). In the case of $4\pi b/V < k^2$ and a sharp interface (between vacuum and medium), the reflectivity is given by the Fresnel expression.

$$R = |r|^2 = \left| \frac{k - k_i}{k + k_i} \right|^2 \tag{35}$$

that, for high value of k, has the limiting form of

$$R \sim \pi^2 \left(\frac{b}{V} \right)^2 \frac{1}{k^4}. \tag{36}$$

The reflectivity of a multilayer stack of thin film can be calculated by the following recursive scheme. For each slab i and $i - 1$, the reflectance denoted by $r_{i-1,i}$ is given by the Fresnel

expression:

$$R = |r|^2 = \left|\frac{k_{i-1} - k_i}{k_{i-1} + k_i}\right|^2. \tag{37}$$

The combined reflectance of the interfaces between the substrate and layer $n-1$, and layer $n-1$ and $n-2$, denoted by $r_{n-2,n}$, is given by the combination of these individual interfaces:

$$r_{n-2,n} = \frac{r_{n-2,n-1} + r_{n-1,n}\mathrm{e}^{2\mathrm{i}k_{n-1}d_{n-1}}}{1 + r_{n-2,n-1}r_{n-1,n}\mathrm{e}^{2\mathrm{i}k_{n-1}d_{n-1}}} \tag{38}$$

where d is the thickness of the slab. By combining this reflectance with the reflectance of the interface between layers $n-3$ and $n-2$ to yield the reflectance of all interfaces from $n-3$ to the substrate, the process can be continued recursively until the top interface is reached and therefore the reflectivity is obtained. This algorithm can be applied to calculate a general profile. By approximating a continuous profile by a stack of such thin layers (normally one chooses layer thickness to give a constant increment in scattering length density between each layer), one can calculate the reflectivity of any profile to the accuracy required within a given k range.

The presence of a diffuse interface causes the reflectivity to fall off more rapidly than k^{-4}; hence, in the case of an interface between two semi-infinite media and if the deviation of the interface from a flat surface can be described by Gaussian statistics, equation (37) can be replaced by [53, 54]

$$R_{\mathrm{R}}(k) = R_{\mathrm{F}}(k)\exp(-4k^2\sigma^2) \tag{39}$$

where $R_{\mathrm{F}}(k)$ is the reflectivity in the absence of composition gradients at the interface.

In systems composed of different polymer layers, each interface could present Gaussian roughness. If n layers are considered, the Fresnel reflection coefficient between the nth and the $(n-1)$th layers defined in equation (37) will be modified such that

$$r_{n,n+1} = \left(\frac{k_n - k_{n+1}}{k_n + k_{n+1}}\right)\exp(-2\sigma_{n+1}^2 k_n k_{n+1}) \tag{40}$$

and a more complicated expression for the reflectivity can be derived [53].

From a measured reflectivity profile it is thus possible to obtain information about the roughness present at surfaces and interfaces. The interfacial profiles of a thin layer between two semi-infinite media, considering the convolution of a sharp interface by a Gaussian smoothing function [53, 54], can be evaluated with the following formula [56], derived using a Gaussian roughness at each interface:

$$\rho(z) = \sum_{i=1}^{n}\frac{\rho_i - \rho_{i+1}}{2}\left(1 + \mathrm{erf}\left(\frac{z - z_i}{\sqrt{2}\sigma_i}\right)\right) \tag{41}$$

where ρ_i, σ_i and z_i are respectively the scattering length density, the roughness and the distance from the surface for layer i. In the absence of roughness the scattering length density profile is represented by a step and the interface is sharp, while if roughness is considered between the air and the layer the scattering length density increases smoothly and the interfacial region is characterized by a well defined width.

The form of the interfacial profile generated by the error function (erf), as defined in equation (41), is similar to the hyperbolic tangent profile predicted by the self-consistent field theory, and presents a similar density gradient at the interface. The roughness evaluated considering this profile is related to the interfacial width w, predicted by a hyperbolic tangent profile, by the following relation [28]:

$$w = \sqrt{\frac{\pi}{2}}\sigma. \tag{42}$$

Reflectivity measurements are very sensitive to small values of roughness, and narrow interfacial widths can be determined with a resolution of a few ångströms. However, there is an upper limit on the values of roughness that can be accurately measured: for very broad interfaces the reflectivity will decay very fast and the precision with which the width can be determined will depend on the angular resolution of the instrument [53, 54].

8. Systems studied: polyolefin blends

The focus of our work will be on systems consisting of blends of polyolefins with different chain architectures. Previously we have done most work on the classic polystyrene and poly(methyl methacrylate) [5, 42, 43]. In the latter system the segment–segment interaction parameter is relatively large, so in our previous work we have been in the so-called strong segregation regime, far away from criticality. Also, because of the large difference in polarizability between the two components, dispersion forces are large in comparison to the likely situation in the polyolefin mixtures; we have already used this system to demonstrate the role of dispersion forces in providing a small wavevector cut-off on the spectrum of thermally excited capillary waves, thus confirming the importance of the role of capillary waves in substantially broadening the intrinsic interface profile [5].

The components of the polyolefin blends are prepared by the anionic polymerization of butadiene, which is subsequently catalytically hydrogenated to produce a fully saturated polyolefin. When butadiene is polymerized addition can take place either in the 1–2 configuration or in the 1–4 configuration; on hydrogenation a poly(1–2 butadiene) will yield poly(ethyl ethylene) while poly(1–4 butadiene) yields poly(ethylene). The relative amounts of 1–4 and 1–2 addition are controlled by the nature of the solvent; the normal non-polar solvents such as cyclohexane produce mostly 1–4 addition, but on adding increased amounts of polar cosolvents such as THF a higher proportion of 1–2 structures are obtained. Thus by varying the solvent in which polymerization takes place random copolymers of ethylene and ethyl ethylene can be produced with any desired copolymer ratio. When copolymers with different copolymer ratios are mixed, there is an unfavourable thermodynamic interaction that depends in a relatively simple way on the two copolymer ratios. This unfavourable interaction arises from local packing considerations, and following a great deal of work on the bulk thermodynamics of these systems by Graessley, Balsara and co-workers in the USA (see [8, 57] and references therein) there is now a predictive framework in place allowing one to calculate with fair accuracy the interaction parameter between any pair of copolymers.

Different conditions of miscibility were then probed by using a wide range of copolymer ratios that were varied from 0.50 to 0.86, while the molecular weight was also varied between 150.000 and 1 M g mol^{-1}. The χ parameter is calculated from the copolymer ratios $\bar{y}$ using the expression proposed by [8, 58–62]:

$$\chi = (a_0 + a_1\bar{y} + a_2\bar{y}^2)(y_2 - y_1)^2 \tag{43}$$

where $\bar{y}$ is the mean copolymer ratio and the coefficients a_0, a_1 and a_2 are linear combinations of the interaction parameters $\chi_{A/B}$, $\chi_{A/A-B}$ and $\chi_{B/A-B}$ (the interactions between homopolymer and copolymer). The values of these coefficients have been determined experimentally for random copolymers of butene and ethylene at different temperatures and are given in [8].

The values of these coefficients at 83 °C are respectively 0.062, −0.114 and 0.220 [8]. The degree of immiscibility χN, where N is the degree of polymerization of the polymers, was then varied from 4.1 to 31.

With these polymer pairs, by continuously tuning the interaction parameters, we can explore the full continuum of situations, from near criticality to strongly immiscible, and for

near critical pairs at high molecular weight, where mean field behaviour is expected, to much smaller molecular weights.

9. Samples preparation and neutron reflectivity experiments

The samples for neutron reflectivity were prepared as follows: bilayers of 50% deuterated and hydrogenated random copolymers were prepared. The substrate was a silicon block (orientation (111)) with a 5 cm diameter and 5 mm thickness, covered by a thin layer of silicon oxide of thickness between 2 and 3 nm. For the experiments the structure of the samples was silicon substrate/deuterated copolymer/hydrogenous copolymer/air (D/H). In this geometry, since the value of the scattering length density of the hydrogenated copolymer is close to zero, there is a small contrast at the top surface between the sample and the air. The sensitivity of the measurement to the presence of a diffuse interface between the two polymers is therefore improved [63]. The bottom deuterated layer of the co-polymer has been spun cast onto silicon substrate from toluene solutions, while the top hydrogenated layer was first spun onto a glass slide and then floated in water and deposited onto the substrate. The samples were then annealed in a vacuum oven for 5 days at a temperature of around 83 °C, well above the glass transition temperature of the polymers, to allow the interfacial width to reach an equilibrium value [64].

Various systems have been studied: in one case we kept fixed the molecular weight (150 000 g mol^{-1} corresponding to a degree of polymerization N of 2500) and different conditions of miscibility were probed by changing the combinations of copolymer ratios, and thus the interaction parameter χ, from 0.0008–0.012, and in another case we selected various values of the interaction parameter in the range 0.0009–0.0022 and changed the average value of N between 2400 and 16 000.

Moreover, systems were probed to approach criticality by varying the molecular weight of the polymers between 100 000 and 900 000 g mol^{-1} for fixed values of the interaction parameter in the range 0.0009–0.0022.

The isotopic substitution H–D may affect the thermodynamic interaction, as observed in previous studies: the resulting χ parameter of the system will be decreased when the blend with the lower copolymer ratio is deuterated, while it will be higher in the other case [61, 62]. However, the error in the determination of the value of χ for the combinations of copolymer ratios used in the experimental work was estimated to be less than 5% [57, 8, 61].

The neutron reflectivity profiles were measured using various reflectometers: D17 at the Institut Max Von Laue–Paul Langevin (Grenoble) [65], CRISP at the Rutherford Appleton Laboratory (UK) [54], V6 at the Hein–Meitner Institute in Berlin (Germany), and the reflectometer AMOR at the Paul Scherrer Institute in Switzerland. The resolution used varied between 3% and 5%.

The reflectivity profiles obtained from the bilayers were then fitted using a silicon/silicon oxide/deuterated polymer/hydrogenated copolymer/air model, with Gaussian roughness at the surface and at the polymer/polymer interface. In this configuration, since the hydrogenated film has a very low scattering length density, there is not much contrast between the air and the top surface of the sample. Thus the reflectivity measurement is not very sensitive to the value of the surface roughness.

The thickness of both the silicon oxide layer and the copolymer films were also previously measured with spectroscopic ellipsometry. The roughness of the SiO_2 layer was fixed to 5 Å, as measured previously in similar silicon crystals [5]. The scattering length density and the surface roughness of the polymers were also determined with neutron reflectivity experiments on single layers and then fixed during the fitting. For deuterated copolymers the value of scattering length

density was around 3×10^{-6} Å^{-2}, while for hydrogenated blends it was found to be between 2×10^{-7} and -3×10^{-7} Å^{-2}. The surface roughness was around 8 Å for all the copolymers, as also measured from AFM experiments [64].

10. Interfaces in polymer systems approaching criticality

To investigate the dependence of the interfacial width on the distance from the critical point, pairs of hydrogenated and partially deuterated copolymers of ethylene and butene were studied with neutron reflectivity. As we have mentioned before, the width of the interface is determined by a balance between the entropy of the system, mainly related to the number of units in the two polymer chains N, and the unfavourable energetic interaction between different monomers described by χ. Thus there are two ways to achieve criticality. For polymer pairs with a small interaction parameter, χ, the critical point occurs at higher molecular weights, while more interacting systems reach criticality at lower N.

In order to understand the relative importance of energetic interactions and entropic effects in determining the interfacial profile, two different sets of experiments have been performed. In the first set the molecular weight has been fixed, and different conditions of miscibility have been probed by changing the combinations of copolymer ratios, and thus the interaction parameter. The values of χ varied between 0.001 and 0.011, while the molecular weight was fixed at four different values in the range 150 000–600 000 g mol^{-1}. In other series of samples, criticality was approached by varying the molecular weight of the polymers between 100 000 and 900 000 g mol^{-1} for fixed values of the interaction parameter in the range 0.0009–0.0023.

The samples have been annealed in a vacuum oven for 5 days at temperatures between 27 and 121 °C well above the glass transition of the two polyolefins [66]. For some samples longer annealing times, up to 12 days, have also been used. Bilayers of random copolymers of ethylene and butene have been prepared following the procedure described in section 4.

The structure of the samples was *silicon substrate/deuterated copolymer/hydrogenous copolymer/air* (D/H). In this geometry, since the value of the scattering length density of the hydrogenated copolymer is close to zero, there is a small contrast at the top surface between the sample and the air, and the sensitivity of the measurement to the presence of a diffuse interface between the two polymers should improve. For some samples, the deuterated film was deposited on top of the hydrogenated film (H/D). Both the layers had a thickness between 2600 and 5000 Å, in order to avoid the presence of confinement effects, which have been observed in thinner films [5, 11].

Figure 1 shows examples of neutron reflectivity profiles measured from D/H bilayers with degree of polymerization $N \sim 2500$ for three different values of χ—0.0112, 0.0033 and 0.0018. All the curves present total reflection up to $q_c \sim 0.0125$ Å^{-1} due to the presence of approximately the same amount of deuterium in the bottom layer. From the figure we can observe that, after the critical edge, the reflectivity profiles fall off more rapidly as the degree of immiscibility χN is decreased, being an indication of a rough interface. This is more pronounced when the interaction parameter χ is decreased from 0.0033 to 0.0018.

From the values of interfacial roughness σ_{INT} found from the fits, the total width of the interface $2w$, as given by a hyperbolic tangent profile, has then been determined with the relation (42). Figure 2 shows the results obtained for polymer pairs with degree of polymerization $N \sim 2500$ and different interaction parameters as a function of the degree of immiscibility χN. The dependence of the interfacial width on the distance from the critical point presents two different behaviours: for degrees of immiscibility higher than 8 the interfacial region increases gradually as the interaction parameter is decreased, while for

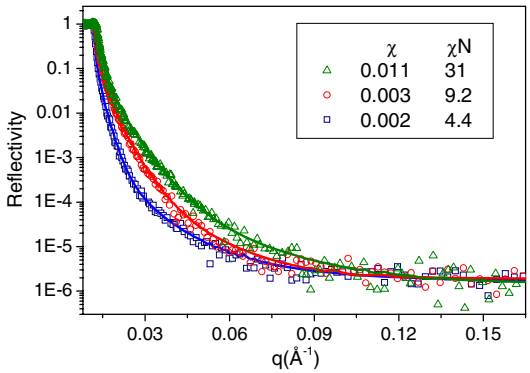

Figure 1. Reflectivity profiles for copolymer pairs with different interaction parameter χ and degree of polymerization $N \sim 2500$ (each layer thickness is between 2600 and 5000 Å and the Kiessig fringes are then unresolved).

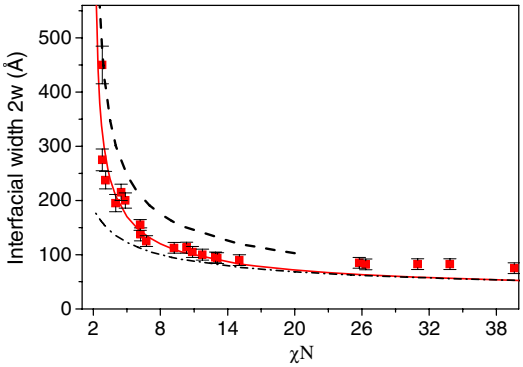

Figure 2. Interfacial width as a function of the degree of immiscibility N for polymer pairs with changing interaction parameter and degree of polymerization $N \sim 2500$. The experimental data are compared to the numerical calculations of the SCF theory (solid line) and to the theoretical predictions in the strong segregation limit (SSL) (dot–dashed line). The dashed line is obtained by using the squared gradient theory in the weak segregation limit (WSL).

$\chi N < 8$ the dependence of the interfacial width on the degree of immiscibility becomes stronger, and the interface starts to diverge [67].

To verify the validity of the analytical expressions for the interfacial width and the interfacial tension in the approximations of strong and weak segregation, the experimental data obtained have been compared with the predictions of the theory in these limits. As reviewed in sections 3 and 4, the self-consistent field theory, in the strong segregation limit, with the additional correction for interfacial fluctuations, should describe the behaviour of the interfacial width for highly immiscible polymers, but when approaching the critical point the predictions of square gradient theory, in the weak segregation limit, should be more accurate.

In order to compare the experimental results to the theoretical predictions the contribution of capillary waves needs to be taken into account. As seen before, the experimental interfacial profile is broadened by thermally excited fluctuations, which give rise to a dependence of the apparent interfacial width on the lateral resolution. Hence the total interfacial width $2w$ can be written as

$$2w = (4w_I^2 + 2\pi\sigma_\varsigma^2)^{1/2}. \tag{44}$$

In equation (44), w_I represents the intrinsic interfacial width while σ_ς^2 is the capillary wave mean dispersion introduced in section 5. In the experiments performed, the lower cut-off for capillary wavevectors q_{min} is introduced by the lateral coherence length of the neutron beam, λ_{cohe}, of approximately 20 μm [5]. The product πw_I has been used as a cut-off for short wavelengths [39, 68]. Thus the contribution of capillary waves to the interfacial width is given by

$$\sigma_\varsigma^2 = \frac{k_B T}{2\pi\gamma} \ln \frac{\lambda_{cohe}}{\pi w_I} \tag{45}$$

where k_B is the Boltzmann constant, T is the temperature and γ is the interfacial tension. In the strong segregation limit (SSL) w_I and γ were determined by using respectively equations (10) and (11), while in the weak segregation limit (WSL) expressions (17) and (18) were used. In the calculation a value of a of 6 Å [11], and an average volume for the monomer unit of 75 Å^3 [57], were considered, while χ has been calculated with equation (43). A theoretical estimation of the interfacial width $2w$ has then been obtained, by using the value estimated for σ_ς^2 with equation (45) in (44).

Figure 2 shows the comparison between the analytical values and the experimental data. At intermediate degrees of immiscibility, for values of χN between 6 and 15, the SSL curve better approximates the data; however, for more immiscible systems the measured interfacial width is broader than the theoretical predictions. As the miscibility between the polymers is increased a transition is observed to a region where analytical expressions cannot be used to predict the interfacial width: the experimental values found for χN between 3 and 6 are between the two theoretical curves. For the lowest values of degrees of immiscibility studied, when the interfacial width starts to diverge, the square gradient theory in the WSL better represents the results.

To make a more quantitative analysis the results have been compared with numerical calculations of the self-consistent field (SCF) theory. Following the mean field approximation, numerical simulations can be used to determine the width of the interface [25] as a function of the degree of miscibility and of the statistical segment length of the polymers a. The interfacial tension can also be determined if the density of the polymers is known. Since the density is taken to be constant, the only model parameter is χN and no knowledge of the equation of state is required [24]. A more detailed account of these calculations can be found in the appendix [23–25].

In the SCF numerical calculations, the width was determined from the order parameter profile $m(z) = \Phi_A(z) - \Phi_B(z)$ following the second moment definition, dm/dz, appropriate for erf profiles:

$$w_m^2 = \frac{\int dz\, (dm/dz) z^2}{\int dz\, (dm/dz)}. \tag{46}$$

It should be pointed out that in the limit $\chi N \to \infty$ (strong segregation limit) the exact solution of the SCF theory is a tanh profile [25]. Even close to the critical point, our SCF profiles are better approximated by tanh profiles than by erf profiles. However, this difference does not significantly affect our results.

Moreover, the second moment definition, equation (46), w_m for the interfacial width differs somewhat from the usual definition of w_I in the theoretical literature, $w_I = |m(\infty)|/(dm/dz)_o$, which is, e.g., used in equations (12) and (17). For tanh profiles the relation is $w_m \sim 0.9 w_I$, and for erf profiles $w_m \sim 0.8 w_I$ (w_{erf} (equation (42)) $\sim 1.1 w_I$ (equation (9)), w_{NR} (equation (39)) $\sim 0.9 w_I$, w_m (equation (46)) $\sim 0.8 * 0.9 * w_I$)

In figure 2 the results have been compared to the experimental data. As displayed in for $N \sim 2500$, the self-consistent field theory well describes the experimental data at low

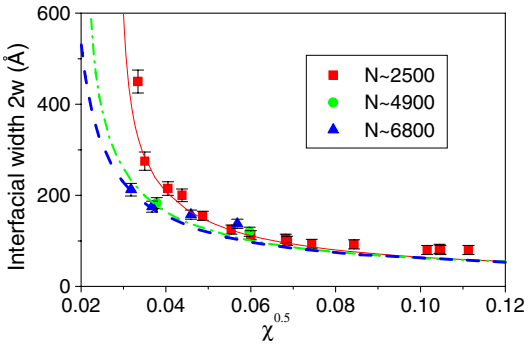

Figure 3. Interfacial width as a function of the interaction parameter χ for series of polymer pairs with fixed degrees of polymerization N. The experimental data are compared to numerical calculations of SCF theory for $N = 2500$ (solid line), $N = 4900$ (dot–dashed line) and $N = 6800$ (dashed line).

values of χ, for $\chi N < 20$. However, for degrees of immiscibility higher than 13, and thus $\chi > 0.005$, the results show discrepancies between experimental data and theoretical calculations. The measured interface is broader than the prediction. However, if the values of the interfacial tension are reduced by approximately 40%, and thus a higher contribution to the interface due to capillary waves is considered, the theoretical predictions describe well the interfacial width also for more immiscible systems. Lower values of interfacial tension were observed by other authors [29] and were confirmed by our experiments on the effect of the confinement approaching criticality [64], where systematically we observed a 40% reduced interfacial tension from the predicted SCF values.

A qualitatively similar behaviour is observed for higher degrees of polymerization, where the divergence from the theoretical predictions at higher values of χ becomes more important. To understand better the effect of the degree of polymerization N on the interfacial width as criticality is approached, in figure 3 the data obtained for the interfacial width for series of polymer pairs with different degrees of polymerization is plotted as a function of the square root of the interaction parameter χ. As can be observed in the figure, at higher values of the interaction parameter χ ($\sqrt{\chi} \geqslant 0.04$) the experimental data collapse.

Thus in this case the degree of polymerization does not affect the interfacial width and the approximation of infinite relative molecular masses is valid. This behaviour also suggests that the discrepancy observed between experimental data and theoretical predictions at higher degrees of immiscibility is not influenced by the molecular weight, but depends only on the interaction parameter χ. For less interacting systems, polymer pairs with higher degree of polymerization show a narrower interface, in agreement with the theoretical predictions. Thus, as criticality is approached, the length of the polymer chains becomes an important factor in determining the divergence of the interface.

For polymer pairs with fixed interaction parameter and varying molecular weights, the dependence of the interfacial width on the degree of polymerization N has also been determined. For these systems, at higher values of χN, as the distance from the critical point is reduced, the interfacial width is almost constant. However, for more miscible polymer pairs, the dependence of the width $2w$ on the molecular weight becomes stronger. Comparing the results obtained for different values of χ, systems with a lower interaction parameter present a wider interface. In particular, for values of χ lower than 0.0014 we observe a good agreement between the experimental data and the SCFT predictions over a wide range of miscibility.

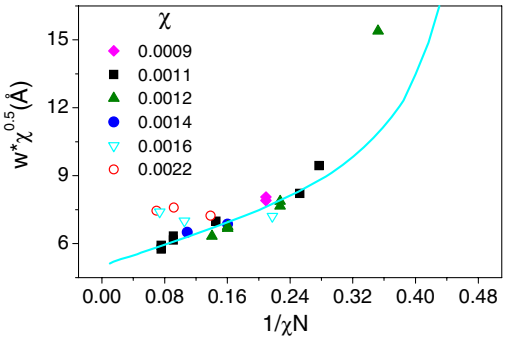

Figure 4. Interfacial width multiplied by $\chi^{1/2}$ as a function of the inverse of the degree of immiscibility for series of polymer pairs with different degrees of polymerization N and fixed interaction parameters. The solid lines are obtained from numerical calculations of SCF theory for $\chi = 0.0012$.

However, for higher values of χ (0.0016 and 0.0022) there is a divergence with the theory at higher molecular weights and the measured interface is broader. This behaviour could be explained again considering a lower interfacial tension, and thus a higher contribution to the interface due to capillary waves, at higher χN. A discrepancy is also observed close to the critical point for χN lower than 3.

These deviations from the theoretical predictions are clearer in figure 4, where the product of the interfacial width with the square root of the interaction parameter has been plotted as a function of the inverse of the degree of immiscibility for all sets of data. Since the interfacial width, for fixed values of χN, depends principally on $\chi^{1/2}$, the theoretical curves representing $2w\ \chi^{1/2}$ as a function of $1/\chi N$ collapse onto a single line. It should be pointed out that the contribution of capillary waves to the interfacial width varies with $\chi^{1/4}$ and not with $\chi^{1/2}$ as the intrinsic width. However, the corrections due to this dependence are very small, as shown when the theoretical curves for different values of χ were calculated. Differences between theory and experimental results are observed only for χ higher than 0.0016 and at very low degrees of immiscibility.

For all the systems studied, the experimental results have shown that as the miscibility is increased the interfacial region becomes broader. For strongly immiscible polymer pairs the width of the interface increases slowly when the degree of immiscibility is decreased. The interfacial width varies in this case only with the interaction parameter χ, and it is independent of the degree of polymerization N of the polymers. Closer to the critical point the dependence on the degree of miscibility is stronger and the way in which the interfacial width diverges, as criticality is approached, is determined by both the interaction parameter of the polymers and the molecular weight. The results have been compared with numerical calculations of the self-consistent field theory. The theory, with the additional contribution due to capillary waves, provides a good prediction of the width of the interface at intermediate values of χ.

11. Confinement effects on fluctuations at interfaces: long ranged and short ranged forces

Polymer molecules in situations of reduced dimensionality often exhibit properties that deviate from those of bulk materials [34]. In thin films, with thickness smaller than a few times the radius of gyration of the molecule, differences in the structural and dynamical properties of the polymers have been observed both experimentally and with simulations [69–73].

These include, for example, changes in the glass transition temperature with decreasing film thickness [69, 70], different chain mobility [71, 72] and a higher compressibility in thinner films [73]. Moreover, it has been shown that effects due to confinement and to molecular interactions in thin film geometry are often responsible for novel physical phenomena. To cite an example, long ranged intermolecular interactions can affect the stability or instability of thin films below a certain thickness [74, 7], leading, in some cases, to spinodal dewetting, and to the formation of patterned structures characterized by a well defined length [75].

Geometric confinement also has an important effect on the interface between two immiscible polymers. Experiments by different groups have shown that the width of the interface between two thin layers depends on the thickness of the films [5, 11, 42–44]. For very thin films the spectrum of capillary waves is modified by the constraint due to the confined geometry, and the measured interfacial width is lower. However, there is a controversy in the literature concerning the relative importance of short and long ranged forces in modifying interfacial fluctuations.

Neutron reflectivity experiments on bilayers of PS/PMMA have shown that for this strongly immiscible polymer pair, when the thickness of the films is thinner than a hundred nanometres, the lower cut-off for the capillary fluctuations is not given by the neutron coherent length, but might be originated by the long ranged van der Waals interactions acting across the films. As a result, in thinner layers the measured interfacial width increases logarithmically with the thickness [5].

For broader interfaces another effect might be considered. The presence of short ranged interactions, i.e. truncation forces due to the cut-off of the interfacial profile by a wall, may introduce another cut-off on the spectrum of capillary waves. Thus, in this case, the measured interfacial width depends strongly on the size of the system and increases with the square root of the film thickness, as observed by nuclear reaction analysis experiments on films of blends of quasi-miscible polymers [11, 44].

Computer simulations on the size dependence of the interfacial profiles between polymeric phases confined between walls have suggested that both these forces in principle should be taken into account [22, 23, 50, 51, 76]. These Monte Carlo studies have shown that the longest wavelengths of capillary waves are determined by a parallel correlation length that incorporates two contributions, a short ranged one due to the distortion of the profile close to the wall and a long ranged one due to Van der Waals interactions. However the interplay of short and long ranged interactions at the interface is still not well understood, and the role of these forces in determining the width of the interface in thin films, as criticality is approached, remains an open question.

The mechanism by which finite size effects influence the interfacial width between two polymers was studied by performing neutron reflectivity experiments on bilayers of polyolefins. Polymer pairs with changing interaction parameter and molecular weight were investigated, to determine how the effect of confinement on interfacial fluctuations depends on the different conditions of miscibility.

To investigate the effect of confinement on the interface between two polymer phases, neutron reflectivity experiments were performed on bilayers of hydrogenated and partially deuterated random copolymers of ethylene and butene, as described previously. The thickness of the top layer was fixed at values between 2500 and 5000 Å, while the thickness of the bottom film was varied in the range 700–9000 Å. To allow the interfacial width to reach an equilibrium state, all the samples were annealed in a vacuum oven for 5 days at about 83 °C, as previously done.

Different conditions of miscibility were probed by using a wide range of copolymer ratios and different molecular weights. In order to understand how van der Waals forces

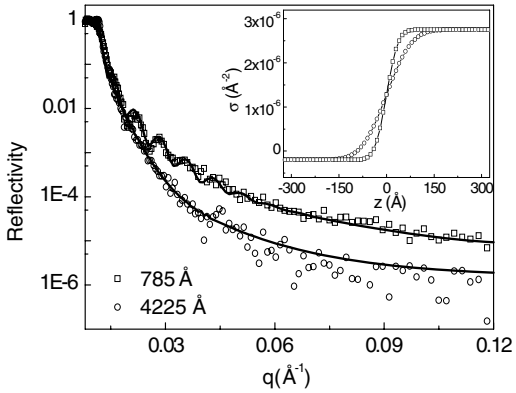

Figure 5. NR of bilayers of polyolefin. The top h-layer (copolymer ratio 86%) was around 4000 Å for both samples while the bottom d-layer (copolymer ratio 70%) was 785 Å (□) and 4225 Å (○). Fits using a three-layer model are shown as lines. In the inset the density profiles extracted from the fits are shown.

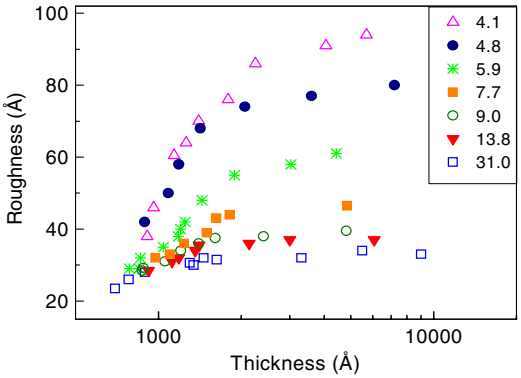

Figure 6. Interfacial roughness as a function of the bottom layer thickness of all the systems measured with NR. The legend shows the different χN values. The fits using the capillary wave model, as described in the text, for the two extreme cases are also shown.

and truncation forces interplay at the interface as the interaction between the polymers is changed, the interfacial width was investigated for combinations of copolymers with interaction parameter χ between 0.011 and 0.002, and with degree of polymerization $N \sim 2500$. Figure 5 shows, as an example, reflectivity curves obtained for polymer pairs with degree of immiscibility of $\chi N = 6.2$, and $N \sim 2500$, for two different thicknesses of the bottom layer: 785 Å (square (red) symbols) and 4225 Å (circular (black) symbols). In the first profile the fringes characteristic of the thickness of the bottom layer are clearly visible. As the thickness of the bottom layer is increased, the fringes disappear and the reflectivity, at values of q bigger than q_c, falls off more rapidly, indicating a wider interface in thicker layers. The density profiles extracted by the fit are shown in the inset.

From the fits of the reflectivity profiles, the interface roughness as a function of the bottom layer thickness was obtained and is shown in figure 6 for various χN.

For all different χN, the roughness increases with the thickness up to a limit value, after which it is stable. By comparing systems with different degrees of immiscibility, it can also be observed that as the layer thickness is increased the interface roughness increases much

faster for weakly immiscible polymer pairs, and the value of the limit thickness at which the interfacial width reaches equilibrium is higher. Moreover, as the degree of immiscibility is decreased and the interface becomes broader, the dependence on the thickness of the bottom layer is stronger.

To understand the relative importance of short and long ranged forces in influencing the width of the interface, a more quantitative analysis is needed. As seen previously, the interfacial roughness σ_{INT} between immiscible polymers can be assumed as the sum of two different contributions:

$$\sigma_{\mathrm{INT}}^2 = \Delta_0^2 + \sigma_\varsigma^2 \tag{47}$$

where Δ_0 is related to the theoretical intrinsic interfacial width w_{I} (as calculated by the self-consistent field theory) by the expression $\Delta_0^2 = 2w_{\mathrm{I}}^2/\pi$, and σ_ς^2 represents the capillary wave contribution to the interface. In the experiments performed on thicker layers, the cut-off for short wavelengths was given by πw_{I} [39], while the lower cut-off for capillary wavevectors $q_{\min}$ is related to the lateral coherence length of the neutron beam, λ_{cohe}, of the order of microns. For thinner films, as reviewed in section 6, external forces affect the spectrum of the capillary waves, introducing a different cut-off for long wavelengths $\lambda_{\max}$ that depends on the thickness of the films. The capillary wave mean square dispersion σ_ς^2 can then be written as follows:

$$\sigma_\varsigma^2(d) = \frac{k_{\mathrm{B}}T}{4\pi\gamma} \ln \frac{(1/\pi w_{\mathrm{I}})^2}{(1/\lambda_{\mathrm{cohe}})^2 + (1/\lambda_{\max})^2} \tag{48}$$

where k_{B} is the Boltzmann constant, T is the temperature and γ is the interfacial tension.

For a thin polymer layer between two semi-infinite media, the dispersion forces acting across the film introduce a dispersive capillary length a_{disp}, given by equation (28).

For the samples studied, since the thickness of the top layer was fixed at several hundred nanometres, while the thickness of the bottom layer was varied, the Hamaker constant in equation (28) represents the dispersion interaction between the top thick layer of polymer and the silicon substrate across the thin bottom film. For small values of d, a_{dis} given by (28) will provide the lower wavevector cut-off $\lambda_{\max}$ in equation (48), leading to a logarithmic dependence of the interfacial roughness on film thickness.

For broader interfaces another effect needs to be taken into account. The short ranged interactions between the surface and the interface modify the interfacial profile. Interfacial fluctuations are then characterized by a large lateral correlation length ξ [46, 49, 77] (given by equation (31)) which increases exponentially with the thickness of the film, d, and can act as a cut-off for long wavelength capillary waves.

The capillary wave mean square dispersion σ_ς^2 can then be calculated, considering that the cut-off $\lambda_{\max}$ of equation (48) is given by ξ of relation (31). As a result, for very thin layers, in the absence of long ranged forces, the contribution of capillary waves to the interfacial width contains a term that is proportional to the square root of the film thickness d.

To determine the relative importance of long and short ranged forces, the experimental data have been fitted to equation (47), where $\lambda_{\max}$ in σ_ς^2 was equal to a_{disp} for the case of long ranged forces and equal to ξ for the short ranged forces. This means that for a thin layer, in the absence of long range forces, the capillary wave mean square dispersion has an expression containing a term that is proportional to the thickness of the film d.

Fixing the neutron lateral coherence length λ_{cohe} to $\sim$20 μm, as previously done [5], for $\chi N \geqslant 9$ the experimental data were in good agreement with the theoretical prediction of a logarithmic dependence on the film thickness characteristic of long ranged forces.

The best fit for $\chi N = 31$, shown in figure 7 at the bottom, is achieved for $\Delta_0 = 20 \pm 3$ Å and $\gamma = (0.93 \pm 0.25)$ mJ m^{-2}. The predictions of the self-consistent field theory (SCFT) for

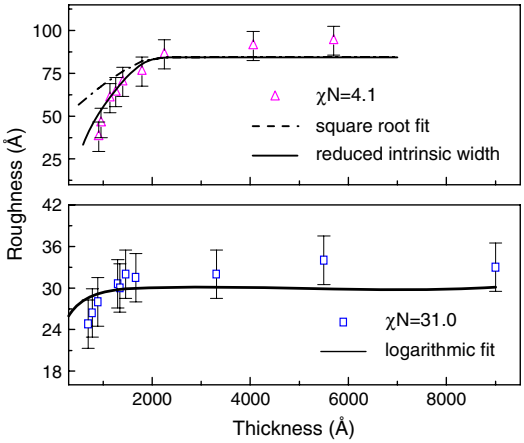

Figure 7. Interfacial roughness as a function of the bottom layer thickness for two systems with $\chi N = 31$ (bottom) and $\chi N = 4.1$ (top). The lines in the top part are fits using equation (48) where $\lambda = \xi$ without (dotted line) and with (solid line) the intrinsic width depending on the thickness. In the bottom part the line is a fit to the experimental data using equation (48) with $\lambda = a_{\text{disp}}$. See the text for details.

Δ_0 and γ in the strong segregation limit are $\Delta_0 = 18$ Å and $\gamma = 1.7$ mJ m^{-2} respectively. For $\chi N = 13.8$, the best fit is obtained for $\Delta_0 = (23 \pm 4)$ Å and $\gamma = (0.77 \pm 0.28)$ mJ m^{-2}, while the predicted values are $\Delta_0 = 24$ Å and $\gamma = 1.3$ mJ m^{-2}. Thus the comparisons of Δ_0 with the theory are good, while the interfacial tensions obtained are in general lower than the predicted values. Similar differences have also been found in numerical self-consistent field calculations and may be related to chain-end effects, as suggested by Werner *et al* [23]. However, the calculated reduction for the interfacial tension (8% for $\chi N = 31$, and 18% for $\chi N = 13.8$) could only partially explain the different results.

The Hamaker constant obtained from the fits was $\sim 5 \times 10^{-20}$ J. This value is larger than the one obtained from calculations based on the Lifshitz theory[4]. For the polymer pair with $\chi N = 31$, by using for the deuterated and the hydrogenated layers respectively the values of refractive index $n_1 = 1.455$ and $n_2 = 1.478$, estimated by ellipsometry measurements, the Hamaker constant found was $\sim 8 \times 10^{-21}$ J. Similar discrepancies have been found in other systems, where the van der Waals interaction between a liquid and a solid substrate through a polymer thin layer deduced from the experiments was higher than the expected value [78]. However, since in equation (48) the Hamaker constant appears inside a logarithm, the results are not very sensitive to the exact value.

For lower degrees of immiscibility and in the region of transition, assuming $\lambda = a_{\text{disp}}$ in equation (1), it is not possible to fit the data. For $\chi N = 4.1$, equation (48) with $\lambda = \xi$ better approximates the experimental data for bottom layer thickness larger than $\sim$1000 Å, as shown in figure 7 (top part).

[4] The non-retarded Hamaker constant between two phases, 1 (silicon substrate in the case considered) and 2 (hydrogenated polyolefin), interacting across a medium 3 (deuterated polyolefin), assumes the following expression [45]:

$$A \sim \frac{3}{4} kT \frac{(\varepsilon_1 - \varepsilon_3)(\varepsilon_2 - \varepsilon_3)}{(\varepsilon_1 + \varepsilon_3)(\varepsilon_2 + \varepsilon_3)} + \frac{3h\nu_e}{8\sqrt{2}} \frac{(n_1^2 - n_3^2)(n_2^2 - n_3^2)}{(n_1^2 + n_3^2)^{1/2}(n_2^2 + n_3^2)^{1/2}[(n_1^2 + n_3^2)^{1/2} + (n_2^2 + n_3^2)^{1/2}]}.$$

By using for the main electronic absorption frequency ν_e the value 3×10^{15} s^{-1} and for the refractive index of the media $n_1 = 3.5$, $n_2 = 1.455$, and $n_3 = 1.478$, a Hamaker constant of 8×10^{-21} J is obtained.

The extrapolated values for Δ_0 and γ are $\Delta_0 = (52 \pm 8)$ Å and $\gamma = (0.09 \pm 0.04)$ mJ m^{-2} respectively, while those for ξ_B, given by equation (32), and k^{-1} are $\xi_B = (69 \pm 8)$ Å and $k^{-1} = (150 \pm 12)$ Å respectively. The obtained value of ξ_B is in good agreement with the theoretical value of 77 Å estimated using the standard mean field approximation [11, 16, 51], and the obtained k^{-1} is also of the same order as the experimental width w—equal to (118 ± 16) Å. For bottom layers thinner than ∼100 nm the dependence of the interfacial roughness on the thickness becomes stronger, as clearly visible in the top part of figure 7. For thin layers of the order of five times the interfacial width, short range forces may affect not only the capillary wave contribution to the interface but also the intrinsic interfacial width. This 'squeezing' of the intrinsic interface has been predicted by Binder *et al* in simulation [50] using a Ginzburg–Landau type theory. In their simulation, preferential attraction of the species for the walls was introduced in the free energy of the film. Using the approach of Binder *et al* [50] in the weak segregation limit, the intrinsic interface should depend on the thickness in the following way:

$$w_I(d) = \frac{w_I(\infty)}{\sqrt{1 + C \cdot \exp(-d/(2 \cdot \xi_B))}} \tag{49}$$

where d is the film thickness, C is a constant related to the parameters characterizing surface interactions and $w_I(\infty)$ is the intrinsic width at larger value of thickness.

Using this expression for the intrinsic width with the capillary wave term as before, we have fitted the data and the following parameters have been obtained: $\Delta_0 = (60 \pm 8)$ Å, $\gamma = (0.06 \pm 0.04)$ mJ m^{-2}, $\xi_B = (69 \pm 8)$ Å, $k^{-1} = (150 \pm 12)$ Å and $C = 50 \pm 20$. Figure 2, top part, also reports this fit obtained (solid line) showing a good agreement also at lower thickness. These parameters are similar to the one reported before and the value of C is slightly higher than but of the same order as the value of 16 predicted theoretically in the weak segregation limit [49]. This result may suggest the need of an additional effect that cannot be explained by a simple Flory–Higgins or SCF theory for a planar slab.

For intermediate values of χN, it is not possible to fit the data assuming $\lambda_{max} = a_{disp}$ or $\lambda_{max} = \xi$. The thickness dependence, in this case, may be due to the effect of both short and long ranged forces. An attempt to describe the experimental results was made assuming simple additivity between the two different interactions, and thus using for $1/\lambda_{max}$ the following expression:

$$\frac{1}{\lambda_{max}} = \frac{1}{a_{disp}} + \frac{1}{\xi}. \tag{50}$$

However, with this approach, previously used in Monte Carlo simulations [23], it was not possible to fit the experimental values obtained for the interfacial roughness for thinner bottom layers. This suggests that the combination of short and long range forces leads to a more complicated dependence of the interfacial width on film thickness.

To investigate the limit of long ranged forces in modifying the spectrum of capillary waves, with an approach that was independent on the parameters chosen for the single fits, a different analysis of the experimental data was also carried out. As observed previously, the capillary wave mean dispersion σ_ζ^2 for thicker bottom layers can be written as

$$\sigma_\zeta^2 = \frac{k_B T}{4\pi\gamma} \ln \frac{(1/\pi w_I)^2}{(1/\lambda_{cohe})^2}. \tag{51}$$

For thin films, if the cut-off for long wavelengths is determined only by long ranged forces, the contribution of capillary waves to the interface is given by

$$\sigma_\zeta^2(d) = \frac{k_B T}{4\pi\gamma} \ln \frac{(1/\pi w_I)^2}{(1/\lambda_{cohe})^2 + (A/4\pi\gamma d^4)}. \tag{52}$$

The difference in capillary wave mean square dispersion between thick and thin layer cases, $\Delta\sigma_\zeta^2$, is then given by the following relation:

$$\sigma_\zeta^2 - \sigma_\zeta^2(d) = \Delta\sigma_\zeta^2 = \frac{k_B T}{4\pi\gamma} \ln \frac{(1/\lambda_{cohe})^2 + (A/4\pi\gamma d^4)}{(1/\lambda_{cohe})^2}. \tag{53}$$

Taking the exponential of both left- and right-hand sides, equation (53) can then be rewritten as

$$\gamma(e^{\Delta\sigma_\zeta^2\gamma/A'} - 1) = A'' \frac{1}{d^4} \tag{54}$$

where A' and A'' are two constants defined as

$$A' = \frac{k_B T}{4\pi} \tag{55}$$

and

$$A'' = \frac{A\lambda_{cohe}^2}{4\pi}. \tag{56}$$

It should be noticed that the Hamaker constant A in equation (56) might not have exactly the same value for the different polymer pairs investigated. However, small changes are expected for the combinations of copolymer ratios used, as also confirmed by measurements of the refractive index for the different copolymers performed by ellipsometry[5].

In equation (54) the right-hand side does not depend on the degree of miscibility, therefore it is possible to introduce a function $F(\gamma, \Delta\sigma_\zeta^2)$ defined as

$$F(\gamma, \Delta\sigma_\zeta^2) = \gamma(e^{\Delta\sigma_\zeta^2\gamma/A'} - 1) \tag{57}$$

that for the different conditions of miscibility studied will vary only with the thickness of the bottom layer d:

$$F(\gamma, \Delta\sigma_\zeta^2) = A'' \frac{1}{d^4}. \tag{58}$$

Making use of relation (47), the quantity $\Delta\sigma_\zeta^2$ can be calculated directly from the experimental data, as the difference between the limit value reached by the interfacial roughness and the values of σ_{INT} measured for different thicknesses of the bottom layers. Thus, by using for the interfacial tension γ the values predicted by numerical calculations of SCF theory (see the appendix), it is possible to calculate the values of $F(\gamma, \Delta\sigma_\zeta^2)$ as a function of the thickness of the layers for the different conditions of miscibility.

In figure 8 the function $F(\gamma, \Delta\sigma_\zeta^2)$, using for the interfacial tension γ the values predicted by numerical calculations of SCF theory, is plotted on a logarithmic scale as a function of $1/d^4$. For χN higher than 6.8 the data collapse to the same values, as shown by the trend line, and the assumption of a logarithmic dependence on the thickness is verified: in this range therefore long ranged forces are dominant in determining the width of the interface. For lower degrees of immiscibility the dependence on the thickness of the bottom layer becomes stronger as the miscibility is increased and the interface is broader. This suggests that in this case short ranged forces are more important in determining the interfacial profile. The same results are obtained if different expressions for the interfacial tension, such as the interpolation formula suggested by Tang and Freed [18] and the values extracted with the approximation given by Werner *et al* [23], are used to calculate $F(\gamma, \Delta\sigma_\zeta^2)$.

[5] By using the formula reported in footnote 4, the values of the Hamaker constant estimated for the copolymer pairs $\chi N = 31$ ($n_2 = 1.463$, and $n_3 = 1.478$) and $\chi N = 9$ ($n_2 = 1.467$, and $n_3 = 1.478$) are respectively $\sim 5 \times 10^{-21}$ J and $\sim 4 \times 10^{-21}$ J.

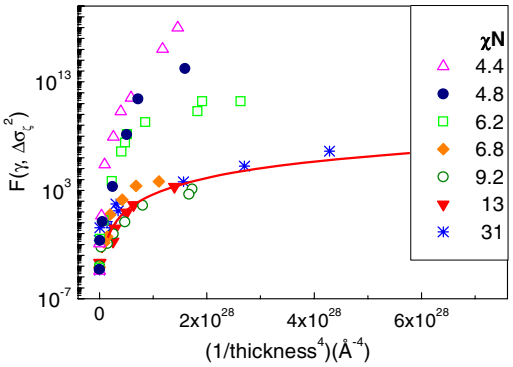

Figure 8. Function $F(\gamma, \Delta\sigma_\varsigma^2)$ defined by equation (58) plotted as a function of (1/bottom layer thickness^4) for different degrees of immiscibility χN. For values of χN higher than 6.8 the data collapse to the same values, as shown by the solid (red) line (guide to the eye), and the assumption of a logarithmic dependence on the thickness is verified.

Our results offer an explanation for the contrasting experimental results obtained in previous studies of interfacial widths between coexisting polymer phases. Kerle *et al* [11, 44] observed a square root dependence on the thickness for a polymer pair rather close to the critical point, while our data showed instead a logarithmic dependence on the thickness for the strongly immiscible polymer pair PS/PMMA [5, 42, 43].

12. Fluctuations at interfaces: chain length effects

One important and open question is to determine what role the molecular weight of the polymers plays in both situations. To probe the effect of a confined geometry on the interface between polymers with different chain lengths, and thus to have a more complete understanding of the dependence of the interfacial width on the thickness in different conditions of miscibility, we investigated here the interface between polymer pairs varying both the molecular weight and the interaction parameter [79].

Figure 9 shows, as an example, reflectivity curves obtained for a polymer pair with interaction parameter $\chi = 0.0016$ and degree of polymerization $N \sim 4520$ for two different thicknesses of the bottom layer: 810 and 3500 Å. The reflection is stronger in the first profile, that shows clearly the fringes due to the presence of a thin bottom layer, while the reflectivity falls off more rapidly as the thickness of the bottom layer is increased, indicating a wider interface in thicker layers. The fits obtained by a least-square fit to a three-layer model (Si/SiO_2/D-polymer/H-polymer) with Gaussian roughness at the surface and at the polymer/polymer interface are also displayed in figure 9.

From the reflectivity profiles obtained, the dependence of the interface roughness on the thickness of the bottom layer has been determined. As previously observed for systems with lower molecular weights, the results showed that the interfacial roughness increases with the thickness up to a limit value, after which it is constant. The mechanism by which finite size effects influence the interface is not determined only by the limit width of the interfacial region, but depends also on the degree of polymerization of the polymers. By comparing systems with different molecular weights and similar interfacial widths in the absence of confinement, the effect of a confined geometry on the interface between polymers with longer chains can be better understood.

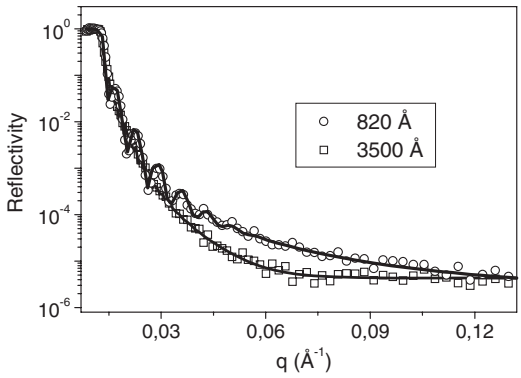

Figure 9. Neutron reflectivity profiles, collected at CRISP, of bilayers of polyolefin with interaction parameter $\chi = 0.0016$ and degree of polymerization $N \sim 4520$. The top hydrogenated layer was around 4000 Å for both samples while the bottom deuterated layer was 810 Å for the circle symbols and 3500 Å for the square symbols. Clearly, the fringes corresponding to the thickness of the bottom layer are visible for the thinner film. The values found from the fits, displayed as solid lines, were respectively (54 ± 5) Å and (68 ± 6) Å.

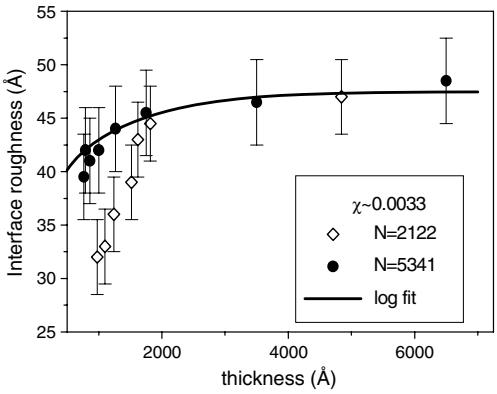

Figure 10. Interface roughness as a function of the bottom layer thickness for polymer pairs with $\chi = 0.0033$ and different degrees of polymerization: $N_1 = 2122$ and $N_2 = 5341$. The solid line is a fit to the experimental data using equation (1), with the lower cut-off for capillary wavevectors $q_{\min}$ defined by the dispersion length a_{disp} and the neutron coherent length λ_{coh}. See the text for details.

In figure 10 the interfacial roughness is plotted as a function of the bottom polymer layer thickness for two cases with both $\chi \sim 0.0033$, while the degrees of polymerization were $N = 2122$ and 5341. The total interfacial width $2w$ found for these systems in the absence of confinement, when both the polymer layers are thick, was ∼117 Å.

As can be observed in figure 10, at higher values of interaction parameter the effect of confinement is stronger for polymer pairs with lower degree of polymerization, and the interface for thinner films is in this case narrower. However, for lower values of the interaction parameter, and thus broader interfaces, the dependence of the interfacial width on the thickness becomes similar and the effect due to a confined geometry is not strongly dependent on the molecular weight of the polymers, as shown in figure 11.

To determine the relative importance of dispersion forces in modifying the spectrum of capillary waves, we tried to fit our data to equation (48), using as the lower cut-off $q_{\min}^2$ the sum

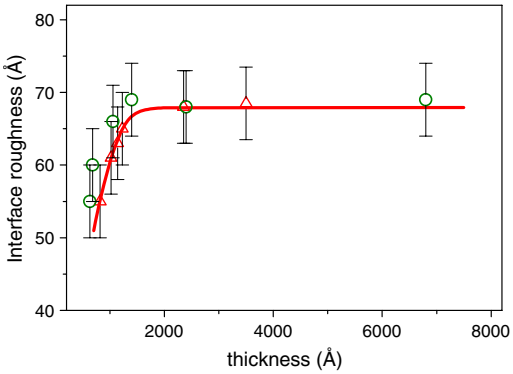

Figure 11. Interface roughness as a function of the bottom layer thickness for polymer pairs with similar equilibrium interfacial widths: $\chi = 0.0014$, $N = 4520$ and $\chi N = 6.2$ (circles) and $\chi = 0.0018$, $N = 10\,246$ and $\chi N = 17.9$ (triangles).

$(2\pi/\lambda_{coh})^2 + (2\pi/a_{disp})^2$, where λ_{coh} is the coherent length in a neutron reflectivity experiment. The experimental data with $N = 5341$ were well approximated by the theoretical prediction of a logarithmic dependence on the film thickness characteristic of long ranged forces, while the polymer pairs with lower molecular weight show a stronger dependence on the thickness.

The best fit, displayed in the figure, is obtained for a value of the Hamaker constant of 8×10^{-20} J, $\lambda_{coh} \sim 29$ μm (similar to the value used in our previous study [5, 42, 43]), $\Delta_0 = (30 \pm 5)$ Å and $\gamma = (0.46 \pm 0.15)$ mJ m^{-2}, while the values predicted by the self-consistent field theory in the strong segregation limit are $\Delta_{0SSL} = 34$ Å and $\gamma_{SSL} = 0.92$ mJ m^{-2}.

As found in previous experiments, Δ_0 is in good agreement with the theoretical prediction, while the interfacial tension obtained experimentally is approximately 40–50% lower then the theoretical one.

For lower values of the interaction parameter, and thus broader interfaces, a different behaviour is observed. The dependence of the interfacial width on the thickness for polymer pairs with different molecular weights becomes similar and the effect due to a confined geometry is not strongly dependent on the molecular weight of the polymers. This is shown in figure 12 where the dependence of roughness on the thickness is displayed for systems with $\chi \sim 0.0016$, and degrees of polymerization $N = 4520$ and 10 246. For both the systems a value of total interfacial roughness $2w$ of approximately 170 Å was found.

As can be observed in the figure, in this case the two series of samples present a similar dependence on film thickness. To make a more quantitative analysis we fit our data to equation (48). Due to the broader interface we are now in the regime where short ranged forces are more important and the lower cut-off q^2_{min} is given by $(2\pi/\lambda_{coh})^2 + (2\pi/\xi)^2$. From the fits, displayed in figure 12 as continuous lines, the following values were found for the different parameters. For both the molecular weights the interfacial tension was $\gamma = (0.16 \pm 0.05)$ mJ m^{-2} and the value obtained for Δ_0 was (43 ± 5) Å. Similar values were also found for the transverse decay length k, $k_1 = (100 \pm 10)$ Å for $N_1 = 4520$ and $k_2 = (95 \pm 10)$ Å for $N_2 = 10\,246$, of the order of the semi interfacial width w of ∼85 Å, while the bulk correlation lengths were respectively $\xi_B = (95 \pm 9)$ Å (calculated value $\xi_B = 102$ Å) and $\xi_B = (162 \pm 12)$ Å ($\xi_B = 172$ Å). At lower values of thickness the fits can be improved if a reduced intrinsic interfacial width is considered (equation (49)). The fits obtained in this case are displayed in the figures as dashed–dot lines: the values found for C are respectively (17 ± 8) for the lower molecular weight, and (8 ± 3) for $N = 10\,246$, of the same order as the value 16 predicted theoretically in the weak segregation limit [50].

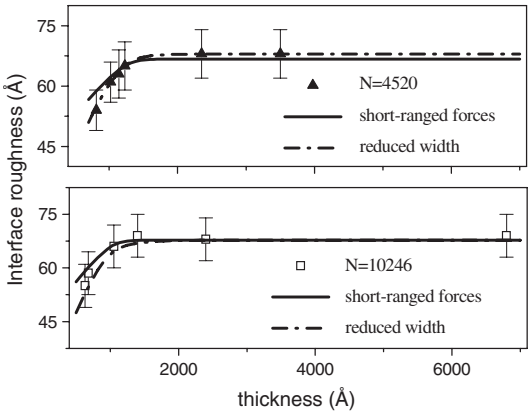

Figure 12. Interface roughness as a function of the bottom layer thickness for polymer pairs with $\chi \sim 0.0016$ for two different values of degree of polymerization: $N_1 = 4520$ (top figure) and $N_2 = 10\,246$ (bottom figure). The solid lines are fits obtained using equation (1), where the lower cut-off $q_{\min}^2$ depends on the neutron coherent length λ_{coh} and on the lateral correlation length ξ introduced by the presence of a short ranged field. The dashed–dot lines are obtained considering also a reduced intrinsic width. See text for details.

The different influence of the chain lengths on the thickness dependence of the interfacial width could be explained considering that polymers with higher molecular weights have a larger bulk correlation length ξ_B. Thus for higher values of χ the short ranged interactions between the surface and the interface will introduce a lateral correlation length ξ that is larger than the dispersive capillary length a_{disp} due to the presence of van der Waals forces. As a result, the cut-off for long wavelength capillary waves is provided by a_{disp}, and the dependence of the interfacial roughness on film thickness for polymer with longer chains is weaker. For polymer pairs with lower interaction parameter short range forces become dominant, and the cut-off for smaller wavevector is determined by the lateral correlation length ξ. Thus the interfacial width increases with the square root of the thickness, and the effect of a higher molecular weight is less important.

As an example, we can consider the case of the polymer pairs with $\chi = 0.0033$ ($N_1 = 2122$ and $N_2 = 5341$). We estimated the bulk correlation length, ξ_B, considering a statistical segment length a of 6 Å [11]. For the first polymer pair we obtained $\xi_B = 65$ Å, while a bulk correlation length of 104 Å was found for the polymer pair with higher N. If a bottom layer of thickness 800 Å is considered, using for k^{-1} a value of 68 Å of the order of the measured semi-interfacial width w of (61 ± 5) Å, the values obtained for the lateral correlation length ξ are $\sim 2\ \mu$m for the polymer pair with $N = 2122$, and $\sim 4\ \mu$m for that with $N = 5431$. The dispersive length a_{dis}, estimated from the fit of the experimental data with the lower molecular weight, is $\sim 2\ \mu$m. Thus, the dependence of the interfacial width on film thickness for systems with longer chains is determined by long ranged forces since ξ is higher than a_{dis}. On the other hand, for systems with $N = 2122$, the values of ξ and a_{dis} are closer and the thickness dependence is given by a combination of long and short ranged forces.

13. Conclusions

Our experiments have clarified important fundamental issues relating to the structure of the interface of very thin polymer films. The experimental effort was focused on a class of polymers

ideally suited for interfacial studies, random copolymers of polyolefins. These systems offer the possibility to tune the interaction parameter of the polymer pair, and thus to control the conditions of miscibility.

For all the systems studied, the experimental results showed that as the miscibility is increased the interface becomes broader. However, two different regimes were found for the dependence of the interfacial width on the distance away from the critical point. For strongly immiscible polymer pairs, the width of the interface increases slowly when the degree of immiscibility is decreased. The interfacial width varies in this case only with the interaction parameter χ, and it is independent of the degree of polymerization N of the polymers. Closer to the critical point the dependence on the degree of miscibility becomes stronger and the way in which the interfacial width diverges, as criticality is approached, is related to the chain length and χ. Our experiments found that the self-consistent field theory numerical calculations, with the additional contribution due to capillary waves, provides a good description of the width of the interface between two polymer bulk phases, in particular at intermediate values of χ. The experimental values of interfacial width were also compared with the analytical expressions derived from mean field theories in the strong and weak segregation limits. At high degrees of immiscibility, the SCF theory, in the strong segregation limit, predicts a narrower interfacial region than the one found in the experiments. Agreement might be obtained if a lower interfacial tension, and thus a higher contribution of capillary waves to the measured width, is considered. For lower χN the interfacial width starts to diverge and there is a crossover to a region of miscibility where the square gradient theory, in the weak segregation limit, better approximates the experimental data.

The thickness dependence of the interfacial width has been studied for different degrees of miscibility, to investigate the effect of confinement on interfacial fluctuations approaching criticality. The results show a gradual transition from a region where long ranged dispersion forces are dominant in influencing the capillary wave spectrum, for higher degrees of immiscibility, to a region where short ranged forces become more important and the dependence of the interfacial width on film thickness is stronger. These results offer an explanation for the contrasting experimental results present in the literature on the thickness dependence of interfacial widths between coexisting polymer phases in a confined geometry, where a square root dependence on the thickness was observed for a polymer pair rather close to the critical point, and a logarithmic dependence on the thickness was instead found for more immiscible polymers. To investigate the effects of a confined geometry on polymers with different chain lengths as criticality is approached, the thickness dependence of the interfacial width for systems with different molecular weights was also studied.

Our results show that far from the critical point, contrary to what has been observed in the absence of confinement, where the interfacial width is independent of the molecular weights of the polymers, the length of the polymer chains has an important role in the determination of the dependence on film thickness. At higher values of the interaction parameter, polymer pairs with a higher degree of polymerization presented, in fact, a wider interface for the same thickness of the bottom film. This can be explained considering that polymers with higher molecular weights have a larger lateral correlation length ξ. Thus van der Waals forces will dominate over short ranged interactions over a wider range of miscibility, and the dependence of the interfacial roughness on film thickness for polymer with longer chains is weaker with respect to lower molecular weight polymers. For smaller χ, and thus broader interfaces, the short ranged interaction between the interface and the other film boundary becomes dominant. As a result the effect due to the finite size is not strongly dependent on the molecular weight and the observed dependence of the interfacial width on the thickness for systems with different degrees of polymerization is similar.

Acknowledgments

We would like to thank RAL Jones and RN Young of the University of Sheffield for their help during all the work, F Schmid of the Universität Bielefeld for theoretical discussion and the SCF calculation and R Cubitt (ILL), R Krastev (HMI), T Gutberlet (PSI) and R Dalgliesh (RAL) for their help during the neutron scattering experiments.

Appendix

The numerical calculations of self-consistent field theory for incompressible binary polymer blends have been performed as indicated by references [24, 25, 23, 22] (we thank F Schmid for providing the calculations).

In these calculations polymer chains are described by continuous curves $R(s)$, where the variable s defines the position along the polymer chain and varies in the range between zero and unity. For an AB blend the effect of the interaction with the other polymer chains is described by the inhomogeneous external potentials U_A and U_B, defined as

$$U_A(r) = \chi\varphi_B(r) + \varsigma(\varphi_A(r) + \varphi_B(r) - 1) \tag{A.1a}$$

$$U_B(r) = \chi\varphi_A(r) + \varsigma(\varphi_A(r) + \varphi_B(r) - 1) \tag{A.1b}$$

where r defines the position in the space, $\varphi_A(r)$ and $\varphi_B(r)$ are the volume fraction profiles, χ is the Flory–Huggins interaction parameter and ζ is an inverse compressibility. In the case of incompressible polymer blends the limit $\varsigma \to \infty$ is considered.

The distribution function of a polymer chain $q_\alpha(r, s)$ (where $\alpha = $ A or B) is given by

$$q_\alpha(r, s) = \int D\{R(s)\} \exp\left[-\frac{1}{6R_g^2}\int_0^s \mathrm{d}s' \left|\frac{\mathrm{d}R(s')}{\mathrm{d}s'}\right|^2 - N\int_0^s \mathrm{d}s'\, U_\alpha(R(s'))\right] \tag{A.2}$$

where R_g is the radius of gyration of the polymers, N is the degree of polymerization and the integral $\int D\{R(s)\}$ considers all the possible configurations for the polymer chain. For simplicity in the numerical calculations the rescaled space unit $r' = r/w_{SSL}$, where w_{SSL} is the intrinsic interfacial width in the strong segregation limit as defined in equation (10), is used. In the case of a planar interface, where only the z' component is important, $q_\alpha(z', s)$ obeys the following diffusion equation:

$$\frac{1}{\chi N}\frac{\partial q_A(z', s)}{\partial s} = \nabla^2 q_A(z', s) - \chi U_A(z') q_A(z', s). \tag{A.3}$$

The volume fractions $\varphi_\alpha(z')$ is then related to the distribution function by the following equation:

$$\varphi_\alpha(z') = \int_0^s \mathrm{d}s\, q_\alpha(z', s) q_\alpha(z', 1 - s). \tag{A.4}$$

Together, equations (A.1), (A.3) and (A.4) form a system of self-consistent equations, which can be solved iteratively until self-consistency is achieved. In the calculations the position of the interface is defined at $z' = 0$ and the following boundary conditions are imposed: at large distance from the interface φ_α assumes the bulk value $\varphi_{\alpha,b}$ and $\varphi_A(z') = \varphi_B(-z')$. To solve the self-consistent problem a mixing scheme is used. Starting in the nth step from an initial guessed potential $U_\alpha^{(n)}(r')$, a new potential $U_\alpha^{(n,\mathrm{new})}(r')$ is obtained by using equations (A.3) and (A.4). The $n + 1$ guess for U_α is then determined by mixing $U_\alpha^{(n)}(r')$ and $U_\alpha^{(n,\mathrm{new})}(r')$ in the following way:

$$U_\alpha^{(n+1)}(r') = U_\alpha^{(n)}(r')(1 - \lambda_n) + -\lambda_n U_\alpha^{(n,\mathrm{new})}(r') \tag{A.5}$$

The mixing parameter λ_n is given by

$$\lambda_n = \min\left(0.1, \sqrt{\frac{\sum_\alpha \int \mathrm{d}r' \,(U_\alpha^{(n)} - U_\alpha^{(n-1)})^2}{\sum_\alpha \int \mathrm{d}r' \,(U_\alpha^{(n,\mathrm{new})} - U_\alpha^{(n-1,\mathrm{new})} - U_\alpha^{(n)} + U_\alpha^{(n-1)})^2}}\right). \tag{A.6}$$

After solving the SCF equations, the intrinsic width of the interface w and the interfacial tension γ are obtained from the volume fraction profiles with the following expressions:

$$w = \frac{\int \mathrm{d}z \left(\frac{\mathrm{d}(\varphi_\mathrm{A}(z) - \varphi_\mathrm{B}(z))}{\mathrm{d}z}\right) z^2}{\int \mathrm{d}z \left(\frac{\mathrm{d}(\varphi_\mathrm{A}(z) - \varphi_\mathrm{B}(z))}{\mathrm{d}z}\right)} \tag{A.7}$$

and

$$\gamma = \gamma_\mathrm{SSL} \int_{-\infty}^{+\infty} \mathrm{d}z' \left((\varphi_\mathrm{A}\varphi_\mathrm{B} - \varphi_{A,b}\varphi_{B,b}) + \frac{\varsigma}{2\chi}[(\varphi_\mathrm{A} + \varphi_\mathrm{B})^2 - (\varphi_{A,b} + \varphi_{B,b})^2]\right) \tag{A.8}$$

where γ_SSL is the interfacial tension in the strong segregation limit.

References

[1] Rowlinson J S and Widom B 1982 *Molecular Theory of Capillarity* (Oxford: Clarendon)
[2] Jones R A L and Richards R W 1999 *Polymers at Surfaces and Interfaces* (Cambridge: Cambridge University Press)
[3] Jones R A L *et al* 1991 *Phys. Rev. Lett.* **66** 1326
[4] Geoghegan M *et al* 1997 *Macromolecules* **30** 4220
[5] Sferrazza M *et al* 1997 *Phys. Rev. Lett.* **78** 3693
[6] Binder K 1999 *Adv. Polym. Sci.* **138** 1
[7] Sferrazza M *et al* 1998 *Phys. Rev. Lett.* **81** 5173
[8] Graessley W W *et al* 1994 *Macromolecules* **27** 3896
[9] Reichart G *et al* 1998 *Macromolecules* **31** 7886
[10] Chaturvedi U K *et al* 1989 *Phys. Rev. Lett.* **63** 616
[11] Kerle T, Klein J and Binder K 1996 *Phys. Rev. Lett.* **77** 1318
[12] Werner A *et al* 1999 *J. Chem. Phys.* **110** 1999
[13] Sanchez I C 1992 *Physics of Polymer Surfaces and Interfaces* (Boston, MA: Butterworth-Heinemann)
[14] Helfand E and Tagami Y 1971 *J. Chem. Phys.* **56** 3592
[15] Cahn J W and Hilliard J E 1958 *J. Chem. Phys.* **28** 258
[16] Binder K 1983 *J. Chem. Phys.* **79** 6387
[17] Broseta D *et al* 1990 *Macromolecules* **23** 132
[18] Tang H and Freed K 1991 *J. Chem. Phys.* **94** 6307
[19] Binder K 1995 *Monte Carlo and Molecular Dynamics Simulations in Polymer Science* (New York: Oxford University Press)
[20] Oslanec R and Brown H R 2003 *Macromolecules* **36** 5839
[21] Budkowski A 1999 *Adv. Polym. Sci.* **148** 1
[22] Werner A *et al* 1997 *J. Chem. Phys.* **107** 8175
[23] Werner A *et al* 1999 *Phys. Rev.* E **59** 728
[24] Schmid F and Muller M 1995 *Macromolecules* **28** 8639
[25] Schmid F 1998 *J. Phys.: Condens. Matter* **10** 8105
[26] Shull K *et al* 1993 *Macromolecules* **26** 3929
[27] Fernandez M L *et al* 1988 *Polymer* **29** 1923
[28] Anastasiadis S P *et al* 1990 *J. Chem. Phys.* **92** 5677
[29] Genzer J and Composto R J 1999 *Polymer* **40** 4223
[30] Guckenbiehl B *et al* 1994 *Physica* B **198** 127
[31] Bucknall D G *et al* 1999 *J. Phys. Chem. Solids* **60** 1273
[32] Bucknall D G *et al* 1998 *Physica* B **243** 1071
[33] Stamm M and Schubert D W 1995 *Annu. Rev. Mater. Sci.* **25** 325
[34] Jones R A L 1999 *Curr. Opin. Colloid Interface Sci.* **4** 153

[35] Helfand E and Sapse A M 1975 *J. Chem. Phys.* **62** 1327
[36] De Gennes P G 1977 *J. Physique Lett.* **38** 355
[37] Schwahn D *et al* 1987 *Phys. Rev. Lett.* **58** 1544
[38] Bates F S *et al* 1990 *Phys. Rev. Lett.* **65** 1863
[39] Semenov A N 1994 *Macromolecules* **27** 2732
[40] Buff F P *et al* 1965 *Phys. Rev. Lett.* **15** 621
[41] Hiester T *et al* 2006 *J. Chem. Phys.* **125** 184701
[42] Sferrazza M *et al* 2001 *J. Phys.: Condens. Matter* **13** 10269
[43] Sferrazza M *et al* 2000 *Phys. Mag. Lett.* **80** 561
[44] Kerle T *et al* 1999 *Eur. Phys. J.* B **7** 401
[45] Israelachvili J 1985 *Intermolecular and Surface Forces* (London: Academic)
[46] Parry A O and Evans R 1990 *Phys. Rev. Lett.* **64** 439
[47] Parry A O and Evans R 1992 *Physica* A **181** 250
[48] Evans R and Parry A O 1989 *J. Phys.: Condens. Matter* **1** 7207
[49] Binder K *et al* 1995 *Phys. Rev.* E **51** 2823
[50] Binder K *et al* 1999 *J. Stat. Phys.* **95** 1045
[51] Binder K *et al* 1994 *Adv. Polym. Sci.* **112** 181
[52] Strobl G 1997 *The Physics of Polymers* (Berlin: Springer)
[53] Russell T P 1990 *Prog. Mater. Sci.* **5** 171
[54] Penfold J and Thomas R K 1990 *J. Phys.: Condens. Matter* **2** 1369
[55] Gragneto-Cusani G 2001 *J. Phys.: Condens. Matter* **13** 4973
[56] Parratt L G 1956 *J. Chem. Phys.* **53** 597
[57] Balsara N P *et al* 1992 *Macromolecules* **25** 6137
[58] Krishnamoorti R *et al* 1994 *Macromolecules* **27** 3073
[59] Krishnamoorti R *et al* 1995 *Macromolecules* **28** 1252
[60] Reichart G *et al* 1998 *Macromolecules* **31** 7886
[61] Graessley W W *et al* 1993 *Macromolecules* **26** 1137
[62] Graessley W W *et al* 1994 *Macromolecules* **27** 2574
[63] Carelli C *et al* 2006 *Nucl. Instrum. Methods Phys. Res.* B **248/1** 170–4
[64] Carelli C *et al* 2005 *Europhys. Lett.* **71** 763–9
[65] Cubitt R and Fragneto G 2002 *Appl. Phys.* A **74** S329
[66] Losch A *et al* 1995 *J. Polym. Sci.* **33** 1821
[67] Carelli C *et al* 2005 *Phys. Rev.* E **72** 031807
[68] Semenov A N 1993 *Macromolecules* **26** 6617
[69] Keddie J *et al* 1994 *Europhys. Lett.* **27** 59
[70] Forrest J A and Jones R A L 2001 *Adv. Colloid Interface Sci.* **94** 167
[71] Brown H R and Russell T P 1996 *Macromolecules* **28** 6808
[72] Binder K *et al* 1996 *Annu. Rev. Mater. Sci.* **26** 107
[73] Varnik F *et al* 2002 *Eur. Phys. J.* E **8** 175
[74] Reiter G 1992 *Phys. Rev. Lett.* **68** 1084
[75] Higgins A M and Jones R A L 2000 *Nature* **404** 476
[76] Werner A *et al* 1999 *J. Chem. Phys.* **110** 1221
[77] Binder K *et al* 1995 *Phys. Rev. Lett.* **74** 298
[78] Reiter G *et al* 1999 *J. Colloid Interface Sci.* **214** 126
[79] Carelli C *et al* 2006 *Europhys. Lett.* **75** 274